OSTBAYERISCHE
TECHNISCHE HOCHSCHULE
REGENSBURG

LABOR FASERVERBUNDTECHNIK

Evaluation of 3D optical motion and deformation analysis using GOM Aramis 6M Essential Line

Anna Adrover i Gili

Bachelor Thesis

Ostbayerische Technische Hochschule Regensburg

Fakultät Maschinenbau

Labor Faserverbundtechnik

Regensburg, September 2018

Ostbayerische Technische Hochschule Regensburg

Fakultät Maschinenbau

Labor Faserverbundtechnik

Evaluation of 3D optical motion and deformation analysis using GOM Aramis 6M Essential Line

Anna Adrover i Gili

Bachelor Thesis

Starting date: 14th March 2018
Due date: 13th September 2018

Examiner: Prof. Dr-Ing. Ingo Ehrlich

Tutor: Marco Siegl, M.Sc

Plagiarisms Statement

1. Mir ist bekannt, dass dieses Exemplar der Bachelorarbeit als Prüfungsleistung in das Eigentum des Freistaates Bayern übergeht.

2. Ich erkläre hiermit, dass die vorliegende Bachelorarbeit selbständig verfasst und noch nicht anderweitig für Prüfungszwecke vorgelegt worden ist, keine anderen als die angegebenen Quellen und Hilfsmittel benützt worden sowie wörtliche und sinngemäße Zitate als solche gekennzeichnet sind.

1. I am aware that this copy of the Bachelor thesis as an examination passes over into the property of the Free State of Bavaria.

2. I hereby declare that this Bachelor thesis is written independently and has not been submitted otherwise for examination purposes, none other sources and aids than those indicated have been used, and verbal as well as analogous citations are marked as such.

Regensburg 12.09.2018 Anna Adrover I Gili

Acknowledgments

First, I would like to express my gratitude to Prof. Dr.-Ing. Ingo Ehrlich for giving me the opportunity to end my Mechanical Engineering studies performing a bachelor thesis at the OTH Regensburg, specifically at the Laboratory of Composite Technology.

Also, I would like to give a special and sincerely thanks to my tutor Mr. Marco Siegl, for the warm welcome, the assistance and the guidance through the entire project.

My grateful thanks are also extended to Mr. Andreas Kastenmeier, Mr. Bastian Jungbauer and Mr. Christian Pongratz for helping me in the setup of the different tests, the manufacture of the necessary specimens and for the comprehension and advice given to me.

Moreover, I truly want to thank my lab partner Aureline Vauge, for always being a great support during the entire project, helping me in every possible occasion.

Finally, I would like to thank the entire group of workers of the Laboratory of Composite Technology for their cooperation whenever it has been necessary.

Abstract

This document provides an overview for the evaluation of the GOM ARAMIS 6M Essential Line (GOM Gmbh, Germany), an optical measurement system that uses digital image correlation to track surface deformation of an object during an experiment and computes the resultant strain data.

Different experimental test methods, such as, a simple cantilever beam test, a tensile test and a 3-Point bending test had been performed to analyse the hardware (resolution, measuring fields and measurement errors), the digital image correlation and the GOM Correlate evaluation software.

The application of the software is done by a 4-point bending test of a fibre-reinforced plastic tube, to determine experimentally its deformation behaviour.

This document presents some key aspects for the use of ARAMIS obtained through the distinct experiments performed.

Key words: Digital image correlation, strain computation, pattern quality, alignment, intersection deviation, calibration, 4-point bending test.

Table of contents

Abbreviations and symbols

Abbreviations

Abbreviations	Meaning
CAD	Computer Aided Design
CS	Coordinate System
DOF	Depth of Field
DIC	Digital Image Correlation
FEM	Finite Element Method
OTH Regensburg	Ostbayerische Technische Hochschule Regensburg
POM	Polyoxymethylene
2D, 3D	Two dimensional, three dimensional
4PBT	4-Point Bending Test
3PBT	3-Point Bending Test

Latin Symbols

Symbol	Meaning
b	Thickness
c	Correlation function
$d\vec{x}$	Differential of the space vector in the current state coordinates.
$d\vec{X}$	Differential of the space vector in material coordinates in the original configuration
E	YOUNG Modulus
$\vec{e}_1$	Unit Cartisian vector (1,0,0)
$\vec{e}_2$	Unit Cartisian vector (0,1,0)
$\vec{e}_3$	Unit Cartisian vector (0,0,1)
$\vec{e}_y$	Global Y axis
$\vec{e}_x$'	Local X axis
$\vec{e}_y$'	Local Y axis
$\vec{e}_z$'	Local Z axis
F	Deformation gradient
F_{ij}	Component of the deformation gradient matrix [F]

$f(x,y)$	Signal of the facet in the original state
$g(x_t,y_t)$	Signal of the deformed facet
h	Width
I	Moment of inertia of the cross-section
l	Length
l_0	Initial length
l_1	Final length
M	Bending moment
$\vec{n}_{LP}$	Local compensation plate
P	Load
p_i	Points of an element
$\overrightarrow{p_i}$	Initial point vector
$\overrightarrow{p'_i}$	Deformed or final point vector
p_0	Initial position of the points
p'_0	Final position of the points
p_x	Initial point position in the x-direction
p_y	Initial point position in the y-direction
p'_x	Deformed or final point position in the x-direction
p'_y	Deformed or final point position in the y-direction
R	Rotation tensor
t	Time
U	Stretch tensor
$\vec{u}$	Displacement vector representing rigid body translation
u_x	Displacement in the x direction
u_y	Displacement in the y direction
V	Original volume of the $d\vec{X}$ element
v	Actual volume of the $d\vec{x}$ element
x	Distance
$\vec{x}$	Position in space
$\vec{X}$	Material coordinates

Greek Symbols

Symbol	Meaning
α	Angle
Δ	Variation
ε	Technical strain
Λ	Stretch ratio
ω	Weighting factor

1.Introduction

The understanding of the deformation behaviour, such as ovalization, of a fibre-reinforced tube is one of the main concerns of the Laboratory of Composite Technology (LFT) of the OTH Regensburg. The aim of the research project regarding the 4-Point Bending Test (4PBT) is to develop an analytical model, which allows to calculate an ovalization of fibre-reinforced tubes and to describe the bending stiffness reduction as a function of deformation. To measure the deformation on the whole surface of the object, the use optical 3-Dimensional (3D) measuring system is required.

GOM ARAMIS is a non-contact optical 3D measuring system that analyses and computes object deformations and dynamic behaviours of the measuring objects [1]. The software is based on the Digital Image Correlation (DIC) working principle. This technique uses as an input a series of digital images taken at different loading steps to determine the changes between the images areas to provide a full-field displacements and localised strain evaluation of an object.

The system computes the 3D coordinates of discrete points over a certain period and compares its initial and final position to evaluate the deformations of the body. The change of position of the referent points allows the software to calculate displacements and strains, as well as derivate quantities such as speed and acceleration.

The determination of the coordinates is possible by means of the stereo camera setup and the application of different types of patterns in the object surface [1]. The patterns can be reference points marks or a stochastic pattern. For the carried-out experiments mostly the stochastic pattern is used, because it is more suitable for the complex evaluations of the strains and displacements that are made.

A system calibration is required to determine the 3D space where the experimental test is taking place. Therefore, the calibration must be done before every measurement.

The DIC technology does have certain limitations that are pointed out in this document. For instance, the most significant limitation is that both cameras must have direct line of sight to obtain paired images for a successful image processing. Different camera positions are arranged for the performance of the distinct test methods to evaluate different working environments in which the GOM ARAMIS can be used.

This document then, proposes diverse working situations or test situations in which the software could be applied and studies more precisely, its suitability for the examination of the tubes on a 4PBT.

2. Goal of the work

The GOM ARAMIS 6M Essential Line is being analysed and evaluated. Different test methods are performed to assets the suitability of the system in distinct environments. The main aim is to understand and inspect the principal characteristics of the software to determine under which conditions the system provides more reliable results of body deformation and strain computation.

Besides a general understanding and study of the hardware functions of the software, analysis of the deformation behaviour of a fibre-reinforced plastic tube is executed. The objective is to determine if the GOM ARAMIS can accomplish reliable and exploitable results, as well as to evaluate its measuring accuracy and performance under diverse configurations.

3. Digital Image Correlation

As it has been introduced, the foundation of the system is the use of Digital Image Correlation (DIC). Therefore, it is important to determine and clarify the main points in which this working principle is based: the evaluation of Image Areas (depending on the pattern applied) and the triangulation.

3.1 Evaluation of Image Areas

Depending on what the user needs to analyse and compute, the applied pattern will differ. If the only magnitude measured is displacements in specific points of the measuring object, then point reference markers should be used. On the other hand, if more detailed and complete analysis of a surface (displacements, strains, velocities among others) is necessary, a stochastic pattern must be applied. However, also a combination of both patterns is possible. In some cases, in which is needed to determine visually an area of inspection, the surface is sprayed with a stochastic pattern and the reference point makers delimitate the area.

3.1.1 Evaluation of Reference Points Markers

Point makers provided by GOM are self-adhesive circular points with a black background and a white centre, creating a high contrast between both colours, as shown in Figure 3.1. In the image pixel transition, the software fits an ellipse in the white spot creating a reference point in its middle. For the point markers identification, the images are locally converted to binary images to determine whether a pixel is displayed in black or white. After this image treatment, the enclosed white areas are located all over the images, can be seen in Figure 3.2.

The detection of the starting points, also named as *point components* by the GOM system, must fit some accuracy parameters. For instance, that the diameter of the reference point makers used fits with the specified in the calibration parameters. Even though another diameter size is being used, the software automatically detects that change and fits the algorithm to evaluate the new diameter.
At least 3 reference point makers are needed to create a point component to evaluate the displacements. Once the starting points are detected, the algorithm of the operating system searches in different directions for distinct gray values on each direction [2]. That way the displacements are computed.

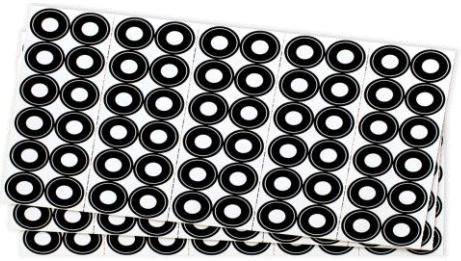

Figure 3.1. Example of a reference point marker[1].

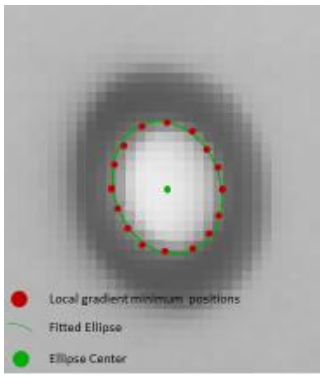

Figure 3.2. Detection of the gray values in the reference point marker [1].

3.1.2 Evaluation of Image Areas via Facets

The key of this paper is to evaluate not only the displacements, but also the strain computation of the GOM system. For this reason, a stochastic pattern must be applied. This random pattern is created from the random application of the points using paint or sprays. With this pattern, the system can clearly relocate the pixels of the camera images (called *facets* by GOM) in all camera images. Due to the full-field approach, the user can analyse the strain behaviour of the part very detailed with a high local resolution [1]. For an optimal measurement, the surface of the measurement object with its pattern must fit the following criteria:

- The surface pattern applied should follow all the deformation of the object and should not break during the image recording.
- The contribution between black and white should be approximately 50/50. This will ensure a good contrast that will lead to a correct detection of the gray values.
- The size of the back spots needs to be adjusted to the measured object dimensions. If the black spots are too small, the software will not be able to use them.
- The flatter the surface of our measuring object, the better the facet identification and 3D point computation.
- The patterns are large enough so that the camera can resolve the patterns completely. Also, the patterns are small enough so that a fine grid of computation facets for the evaluation is available [1].

The application of an ideal stochastic pattern should be like shown in Figure 3.3.

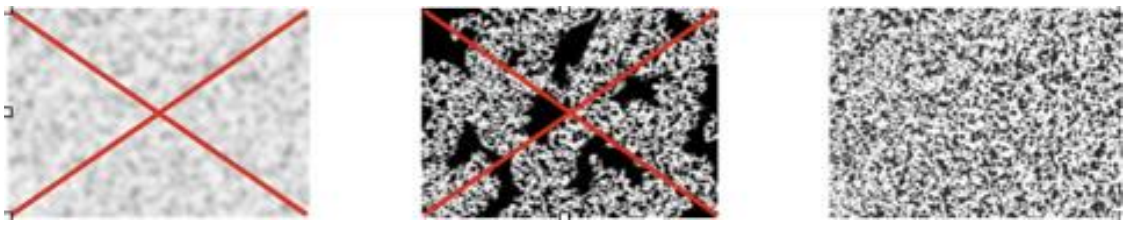

Figure 3.3. Correct application of a stochastic patternt [1].

At first you must make a priming coat with white spray to get the best contrast between black and white, because your measuring object could have a differing surface colour.

It is recommended for its application to practice before the pattern on a paper or another material that can be destroyed. At the beginning, the spray should be pointing at a spot next to the measuring object. When the desired pressure and spray intensity is reached, the spray must be directed to the object.

Once the pattern is applied, the evaluation of the image area via facets by the software begins. It is based on the system of gray value correlation.

The two cameras simultaneously acquire digital images of the stochastic pattern of gray values applied to the sample. In the initial state, the software subdivides the surface into a grid of subsets (square group of pixels). These squares are named *facets*, and their properties can be set in the software by the user in size and distance from each other. Each of these facets represents its centre point which is used as identification point through the several images. When this identification occurs, a facet matching takes place. The deformation of the facet, see Figure 3.4, can calculate strains and displacements.

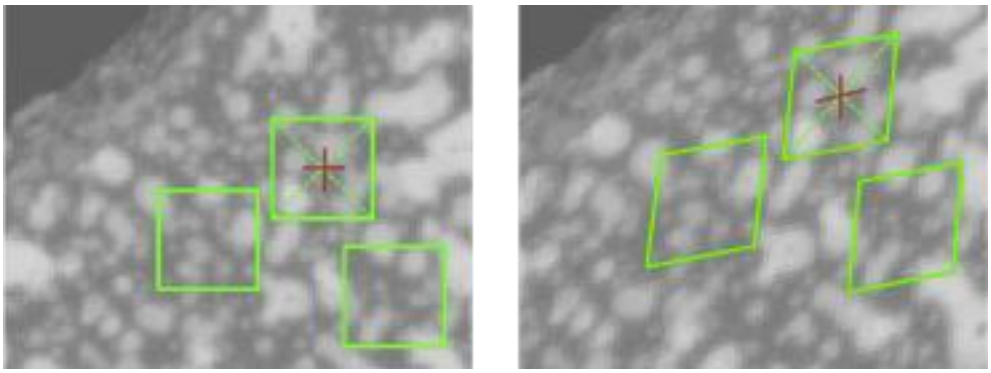

Figure 3.4. Facet detection on a stochastic pattern [2].

The application of the stochastic pattern and so, the random distribution of image information ensures that one facet can be identified as clearly as possible in its immediate environment [1]. The fact that a random pattern is repeated in a random environment is very unlikely, since with a facet size of 19 x 19 pixels and 256 gray values, a variety of 25619 x 19 results exists [1].

The unambiguous identification of deforming image areas is done by means of the image correlation or the method of minimizing deviation squares. The fundamental assumption is that there is a causal relationship between the initial state and the state of deformation. Thus, the program can determine the similarity of two subsets of pixels (facets and search area) at different examined locations and with different displacements.

The rate of similarity between the two signals is done according to the following formula:

$$f(x,y) \leftrightarrow g(x_t, y_t), \tag{3.1}$$

$$c\,(\Delta x, \Delta y) = \frac{\{f(x,y), g(x+\Delta x, y+\Delta y)\}}{|f(x,y)| * |g(x,y)|}, \tag{3.2}$$

where Δx and Δy are the displacements in the *x* and *y* direction respectively.

3.2. Triangulation

DIC is based on photogrammetry basics with foundation relays on triangulation. The software needs two or more signals coming from a point in order to compute a point of origin. By means of the optical sensors and using the information of the sensor calibration, ARAMIS determines the spatial coordinates of the origin from the corresponding image points. The 2D coordinates of a facet, observed from the left camera and the 2D coordinates of the same facet, observed from the right camera, lead to a common 3D coordinate.

It is very important in order to settle an accurate triangulation that allows the system to compute the 3D coordinate (depth), to take into account the intrinsic and the extrinsic parameters. The intrinsic parameters are the camera internal specifications such as: image constants, coordinates of main image point or lens distortion. On the other hand, the extrinsic parameters are those referred to the external orientation and the camera position in the global coordinate system. In Figure 3.5, the principle of triangulation is summarized in a schematic way in which is possible to see the orientation of the cameras (extrinsic parameter).

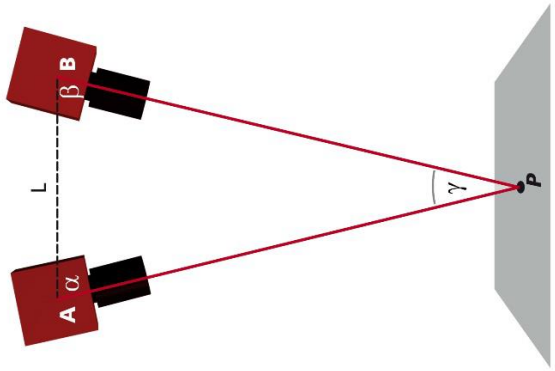

Figure 3.5. Principle of triangulation [3].

4. Strain Computation

In this section, the current method operated by GOM ARAMIS to compute the strains is descripted. A brief introduction about the theoretical calculation of the strains is made, followed by a basic explanation of continuum mechanics and the stretch tensor and how the displayed strain results are obtained by the software.

4.1 Theoretical definitions

To be able to understand future subsections of this chapter, it is necessary to know how the strain and the stretch ratio are related. A strain ε is defined as the relative change of length of an element, and the stretch ratio Λ is the quotient between the final length and the initial length [3]. Thus, the stretch ratio contains the strain, as it is shown in the following formulas

$$\varepsilon = \frac{\Delta l}{l_0}, \tag{4.1}$$

$$\Lambda = \frac{l_1}{l_0} = \frac{l_0 + \Delta l}{l_0} = 1 + \varepsilon. \tag{4.2}$$

A schematic representation of the difference between the length before the deformation l_0, and the length after the deformation l_1, can be shown in Figure 4.1.

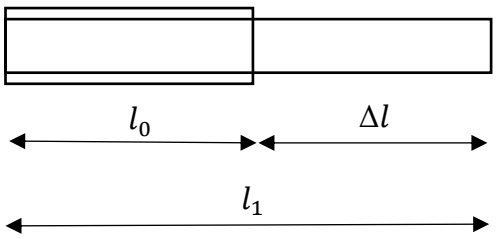

Figure 4.1. Schematic representation of the initial and final length..

4.2 Stretch Tensor

The computation of the stretch tensor arises from continuum mechanics, which is the kinematic and mechanical analysis of a body when deformed. The materials modelled as a continuous mass.
The deformation and motion of a body is described as a change in the shape of the object from a non-deformed or reference configuration to a deformed or final configuration, over a period of time. Over this period, the material body will occupy different configuration at different times so that the particles fill a series of points in space describing a path line [3].
The theoretical explanation can be summarized in the following equation

$$\vec{x} = \chi\left(\vec{X}, t\right) \tag{4.3}$$

where $\vec{x}$ stands for the position in space, *t* for the time and $\vec{X}$ for the material coordinates in the initial or reference configuration that can be described using the Cartesian unit vectors $(\vec{e}_1, \vec{e}_2, \vec{e}_3)$.
As the change of a function in space is its gradient, the deformation gradient F can be expressed as follows:

$$\mathrm{F} := grad\left(\chi\left(\vec{X}, t\right)\right) = \frac{d\chi_i}{d\mathrm{X}_j}\vec{e}_i \otimes \vec{e}_j = \begin{pmatrix} F_{11} & F_{12} & F_{13} \\ F_{21} & F_{22} & F_{23} \\ F_{31} & F_{32} & F_{33} \end{pmatrix}. \tag{4.4}$$

F can be as well named material deformation gradient or GREEN-LAGRANGE strain tensor, because the differentiation takes place at the material coordinates. It can also be considered as a conversion of an element $d\vec{X}$ to $d\vec{x}$ in this way:

$$d\vec{x} = \mathrm{F} \cdot d\vec{X}. \tag{4.5}$$

The dX element, which an original volume *V*, is transformed by means of the F gradient into dx, which has an actual volume *v* [3]. As the material does not change with constant state of aggregation, the inversion and polar decomposition can be applied to deformation gradient tensor F [3]. The tensor, can be split into two new tensors, the rotation tensor R and the stretch tensor U, in the relation

$$\mathrm{F} = \mathrm{R} \cdot \mathrm{U}. \tag{4.6}$$

During the transformation of the points from the original state to the actual state, the stretch is carried out first and afterward the stretched points are rotated. Thus, it is possible to eliminate the rotation tensor so that just the stretch tensor is computed. The resulting stretch tensor is symmetric and positive and contains the stretch ratios and thus, the strains, as can be seen in the following equation:

$$U = \begin{pmatrix} U_{11} & U_{12} & U_{13} \\ U_{21} & U_{22} & U_{23} \\ U_{31} & U_{32} & U_{33} \end{pmatrix} = \begin{pmatrix} \Lambda_{11} & \Lambda_{12} & \Lambda_{13} \\ \Lambda_{21} & \Lambda_{22} & \Lambda_{23} \\ \Lambda_{31} & \Lambda_{32} & \Lambda_{33} \end{pmatrix}. \tag{4.7}$$

4.3 Strain Computation with GOM ARAMIS

In the software there is always a global Coordinate System (CS) which initial position is determined during the first calibration image by means of the position of the calibration panel. Further transformations of the orientation and positioning of the CS are possible and described in the next chapter.
Since the strains in X direction are always in material (local) coordinates moving with the material, each point has its own coordinate system. Thus, the software calculates the expansions of the distances in the moving coordinate systems instead of in the global coordinate system.
For a defined global CS, GOM determines the local axis of the points using the normal of a local compensation plane ($\vec{n}_{LP}$) around the respective point as Z direction to create the local Z axis ($\vec{e}_z$') [3]. After that, the representation of the local X axis results from the cross product of the global Y axis ($\vec{e}_y$) and the normal vector ($\vec{n}_{LP}$). Finally, the local Y axis results from the cross product of the two previous calculated axis.

Summarizing, the distribution of the local KOS is done from this expression:

$$(\vec{e}_z\text{'}) = (\vec{n}_{LP}), \tag{4.8}$$
$$(\vec{e}_x\text{'}) = (\vec{e}_y) \times (\vec{n}_{LP}), \tag{4.9}$$
$$(\vec{e}_y\text{'}) = (\vec{e}_x\text{'}) \times (\vec{e}_z\text{'}). \tag{4.10}$$

A graphical description of how this is applied in a cylindrical body is presented in Figure 4.2.

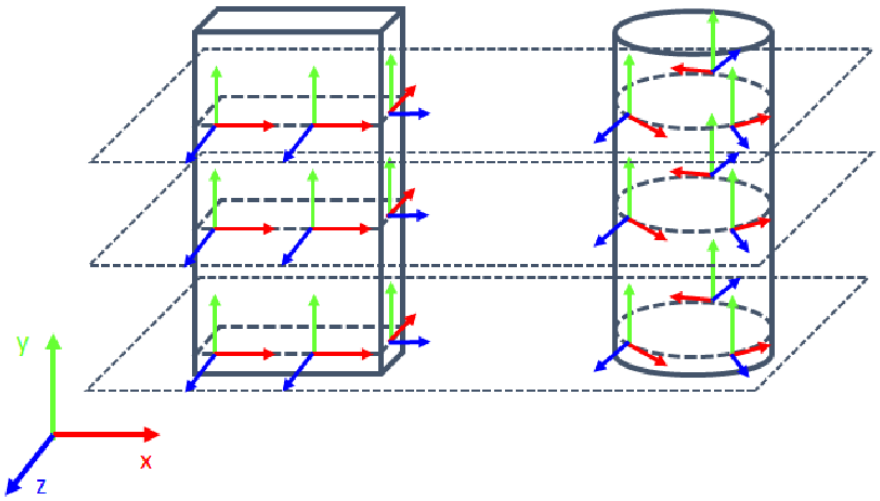

Figure 4.2. Schematic distribution of local coordinate system [3].

The system determines the points on the surface from which the surface strains can be computed. On this surface, the movement of an element can be taken into consideration using as a displacement vector $\vec{u}$, which represents the rigid body translation [3]. The movement and deformation of an element which consists of points p_i is described using the following equation:

$$\overrightarrow{p'_i} = \vec{u} + \mathrm{F} \cdot \overrightarrow{p_i}\,. \tag{4.11}$$

The application of this formula in the computation of the points in the 2D surface results into the following expression:

$$\begin{pmatrix} p'_x \\ p'_y \end{pmatrix} = \begin{pmatrix} u_x \\ u_y \end{pmatrix} + \begin{pmatrix} F_{11} & F_{12} \\ F_{13} & F_{14} \end{pmatrix} \cdot \begin{pmatrix} p_x \\ p_y \end{pmatrix}. \tag{4.12}$$

This equation has 6 unknowns. Therefore, to solve it is needed to know at least the information about the undeformed and deformed coordinates of three points. Theoretically one triangle is enough for computing a strain. However, to reach a better computation and support of the individual measurement points, GOM uses further adjacent points (hexagons) to create an overdetermined system of equations, as shown in Figure 4.3.

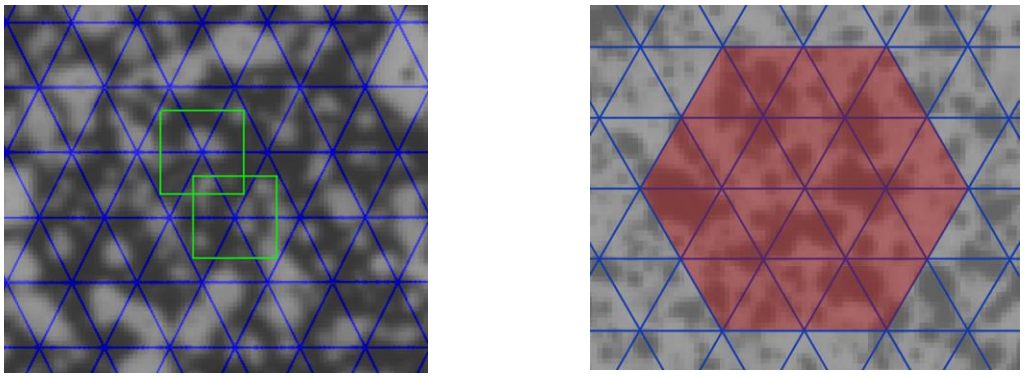

Figure 4.3. Representation of the topology used for the strain [8],[3].

The resulting 2D tensor computed on the surface represents the strains in the surface surrounded by the equilateral hexagon.
There are many points involved in this computation with different density and placed at different distances from the centre of the respective surface [3]. These considerations are considered, giving to the points a weighting factor ω which represents both factors. Then, the overdetermined system of equation can be solved by means of the iterative minimization of the equation

$$\min \sum_{i=1}^{n} \omega_i \, \| p'_i - \mathrm{F} \cdot p_i \, \|^2 \quad . \tag{4.13}$$

From the material coordinates of the different deformation states of a point in which the strain is being calculated can be also used for defining the displacement, as follows:

$$p'_0 = p_0 + \overrightarrow{u}, \tag{4.14}$$

$$\vec{u} = p'_0 - p_0. \tag{4.15}$$

5. General Working Procedure

The ARAMIS system provides the user two different but related software: GOM Snap and GOM Correlate. The first one is used for sensor calibration and image recording, whereas the other is used for displacements and strain computations.

In this section both programs are explained and detailed so that the following chapter, where the evaluation test are described, can be understood.

5.1 GOM Snap

5.1.1. Sensor Setup and Plate Calibration

Before any calculation or computation, it´s required to set up the sensor calibration. Therefore, in this step the use of GOM Snap is necessary.

Part of the triangulation requirements are based on the sensor set up. That is one of the main issues of the system and it is appropriated to set it up anytime an experiment is being handled. The senor calibration is directly dependent on the measuring volume used and the distance where the sensor is positioned from the object.

It is important to clarify some parameters involved in the calibration process, such as: measuring distance, slider distance and aperture. The slider distance refers to the distance between each camera and the middle of the sensor. The measuring distance is the distance between the sensor and the centre of the calibration object. Finally, the aperture is the parameter that regulates the amount of light that passes onto the film during the exposure process. Higher values of aperture mean less opening and so less lightning.
In the upcoming Figure 5.1, the slider distance and the measuring distance are displayed.

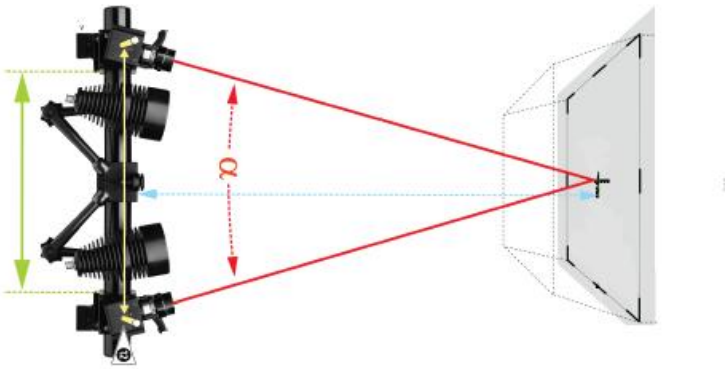

Figure 5.1. Representation of the slider distance (green) and measuring distance (blue) from the top view [2].

For calibrating, two different calibration objects are provided. As one is bigger than the other, they will be further named as Small Plate and Big Plate. According to the information provided by the ARAMIS manual [2], the main or recommended configuration for those plates is the following:

Table 1. Calibration Parameters from GOM Manual [2].

	Small Plate	**Big Plate**
Calibration Object	CP40/MV170	CP40/MV320
Measuring Volume (mm^3) (Weight x Height x Field)	150x120x90	330x270x200
Slider distance (mm)	115	270
Measuring Distance (mm)	340	690
Aperture	11	8
Camera angle (º)	25	25

Depending on the measuring volume that wants to be inspected and the distance that wants to be used, with the same camera lenses, an interpolation of the values can be done. For instance, if the needed and achievable distance is not determined in the table, a new calibration can be settled interpolating the values from the reference table. However, it is very important to consider that after changing those parameters, the aperture may need to be readjusted. In case that the final distance is really close to the original distance, the same aperture can be used, due to the depth of field. The depth of field (DOF) determines how close or further the object can be from the camera. This distance is available in each calibration protocol generated, in the measuring volume dimensions. The measuring distance can then be computed as 40 % of the DOF front and 60 % of the DOF back. For instance, with a measuring distance of 690 mm and a DOF of 200 mm, the system can record images in a range from 610 mm to 810 mm, as indicated in Figure 5.2.

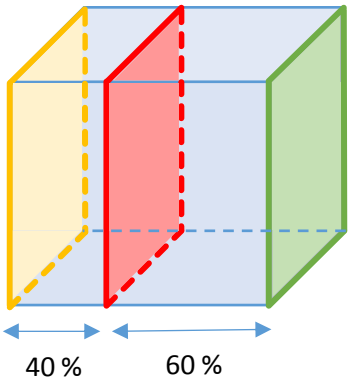

Figure 5.2. Schematic representation of the resulting measuring volume and the range of the DOF. The red plate represents the original position of the object. The yellow plate shows the resulting position of the object moving forward. The green plate shows the final backwards position of the object.

The initial step for the proper calibration is to set up the sensor, clicking in the icons shown in Figure 5.3.

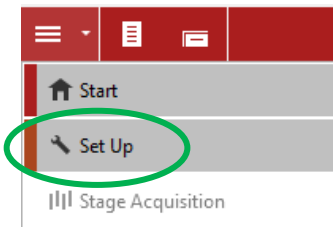

Figure 5.3 Illustration of the location of the set up icon to start the calibration.

Then, the measuring distance and slider distance must be adjusted. The camera position arrangement is made regarding the small and large handle, indicated in Figure 5.3.

Figure 5.3. The large handle is used to move the cameras in radial direction in a limited way.

Once the slider distance is correct, the user must move the camera position, losing the screw located at the back of the camera, so that both lenses point at the middle of the calibration plate, as is exhibit in Figure 5.4 and Figure 5.5.

Figure 13. Location of the back screw that allows the adjustment of the camera angle.

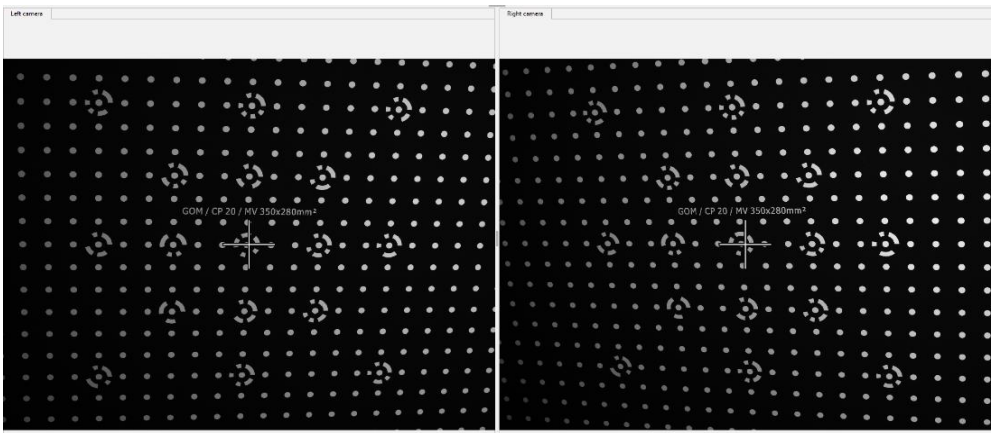

Figure 5.5. Example of a sensor calibration where the left and right cameras pointing at the same center point.

The next step will be adjusting the focus and aperture of the lenses. For the focus adjustment, the user may unlock the screw that blocks the ring (indicated in Figure 5.6) and rotate the focus ring until the letters shown on the calibration plate are perfectly viewable. To ensure that the value is the optimal, the user can check it numerically on the option *Focus Right/Left Camera*, if the optimal focus for the current lighting conditions is achieved.

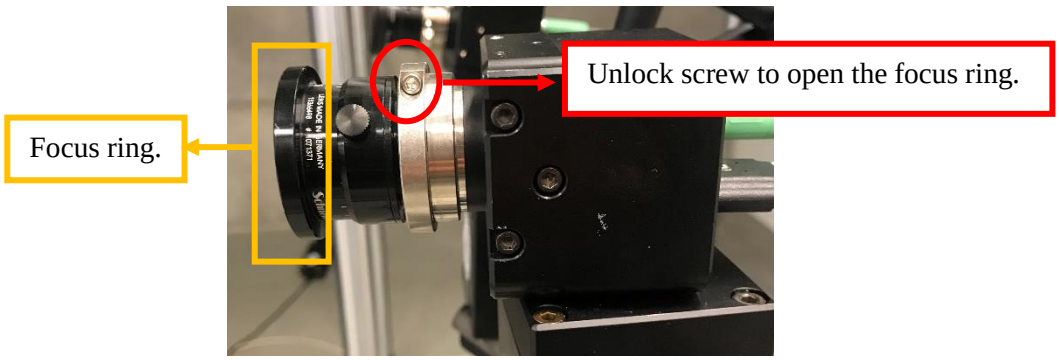

Figure 5.6. Location of the screw and focus ring on the lense.

To adjust the aperture, we need to place a blank paper that covers the plate and switch the live view to a false colour representation (using the right mouse button). Then we need to fix the corresponding aperture, see Figure 5.7, for each plate so that both images (right and left camera) look similar, as displayed in Figure 5.8.

Figure 5.7. Apperture values showed in the lenses. Top view of the lense.

Figure 5.8. Left and right cameras with similar colors representation.

Afterward, 15 minutes warm up is needed before the last step.

The last step is the calibration of the plate itself. First it is asked to choose over which plate (big or small one) the calibration is taking place and later the instructions must be followed.

In this upcoming calibration procedure, the screen of the program displays four areas of interest (blue, green, yellow and red), as can be seen in Figure 5.9.

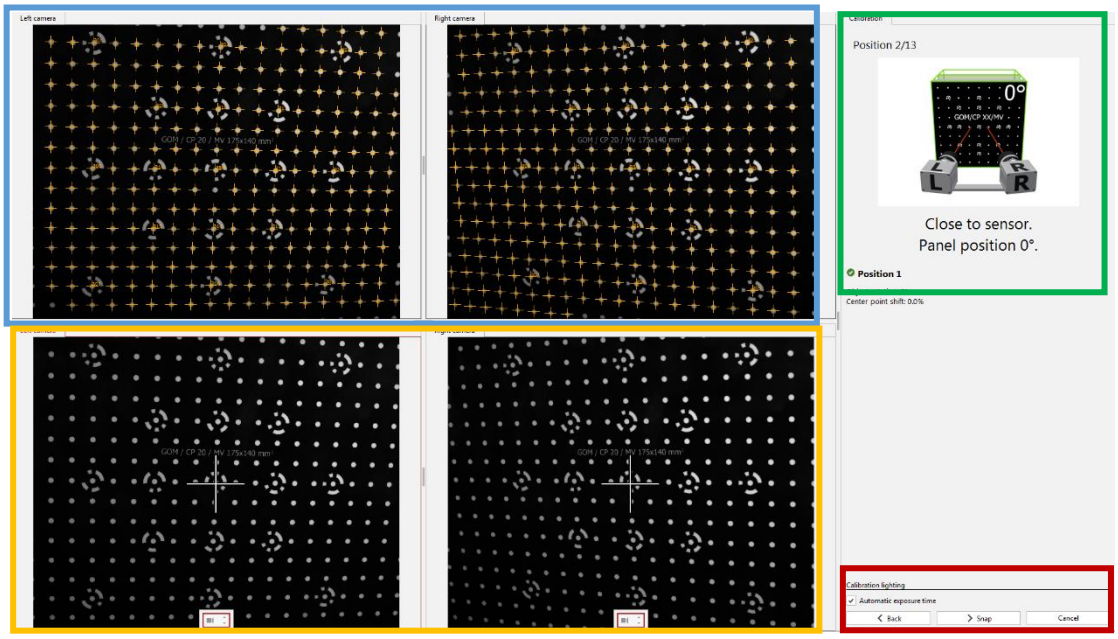

Figure 5.9. Screenshot of GOM Snap calibration procedure, after the first position was arranged. The four main areas of interest are higlighted in different colours.

The green highlighted area in Figure 5.9, individually pictured in Figure 5.10, represents the instructions that the software gives during the process. It shows the required position of the panel, indicating if it has to be rotated or if it has to be drove closer or far away from the sensor. Also, the red lines represent the line of vision of the cameras. In other words, they illustrate where the cameras must be pointing. Moreover, in this area of the screen it is shown the result of the last step, if it was successful or not, and the orientation of the plate.

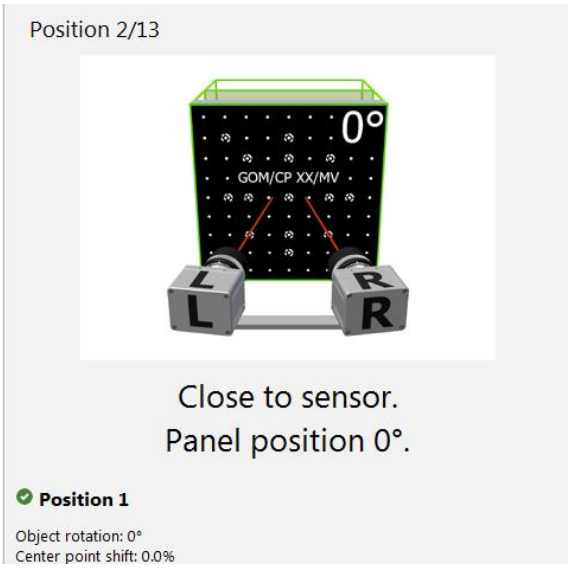

Figure 5.10. Detailed view of the green area indicate in Figure 18. The information regarding the previous position and the second needed position are displayed.

The initial position of the calibration plate is at the determined measuring distance and without any plate rotation, as can be observed in Figure 5.11 and Figure 5.12.

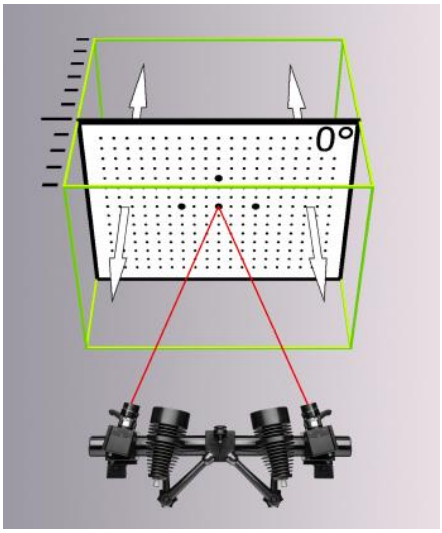

Figure 5.11. First position of the calibration panel in the measuring volume [2].

Figure 5.12. First position of the big plate calibration that was used for the tensile test experiment.

In the first snap taken, in addition to the object rotation information, the software also indicates the centre point shift, as seen in Figure 5.10. The centre point shift determines the deviation between the two initial centre points. A centre shift of 0,0 % means that the two cameras are pointing exactly at the same centre point.

In the bottom part, accentuated in yellow in Figure 5.9 and now showed in Figure 5.13, the software shows the live view of the centre point position in both cameras. It is used to know if the cameras are pointing at the correct spot.

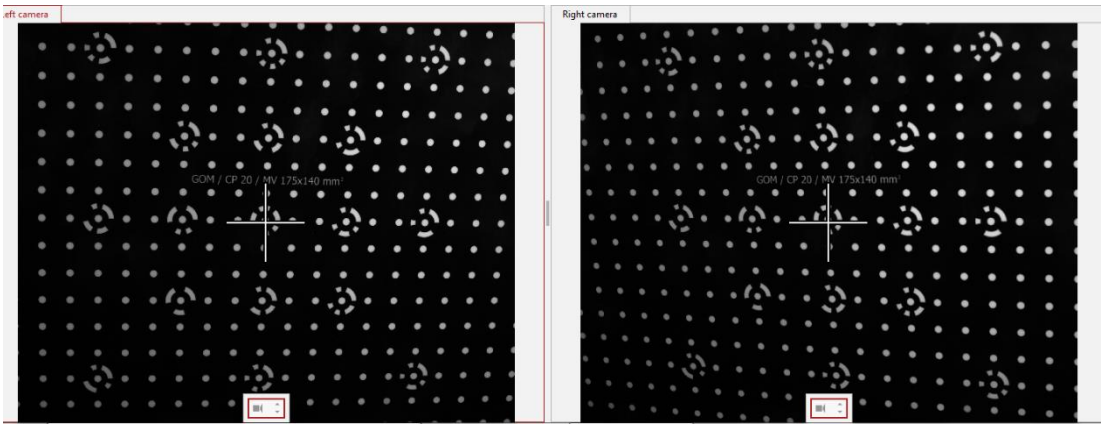

Figure 5.13. Live views of left and right camera at the same time in which both of them are pointing at the same centre point.

When the appropriate position is reached, the user must click on the "snap" bottom, exhibit in the red area in Figure 5.9 and particularly in Figure 5.14. It is recommended to enable the automatic time exposure during the procedure. Also, as can be seen in Figure 5.15, it is possible to go back to a previous position if the result is not satisfying.

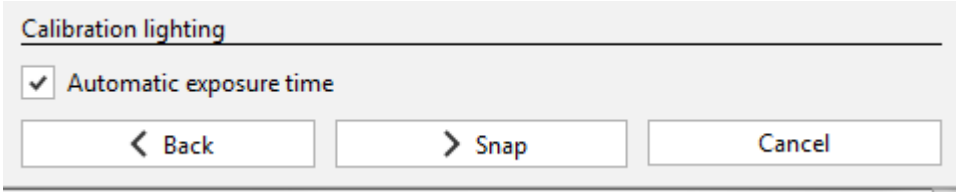

Figure 5.14 Tools that allow you to continue with the process, go back and cancel the calibration process.

After "snap" has been clicked, a picture of the calibration plate is taken and showed in the top site of the screen, precisely seen in Figure 5.15. Here, it can be observed how the software recognize the points of the calibration plate.

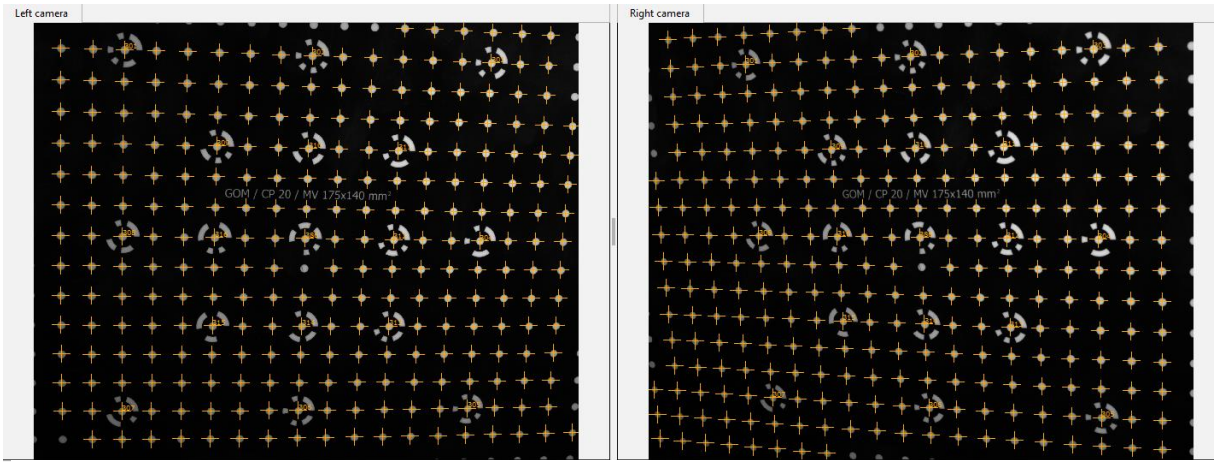

Figure 5.15. Correct recognition of the reference points in the calibration plate by the software in both cameras.

During this procedure is it forbidden to change the cameras position or angle. However, a change in the high of the cameras is needed to complete the process. More precisely, in position four, the calibration plate has to be title 40°, as seen in Figure 5.16 and Figure 5.17.

Figure 5.16. Fourth position of the calibration plate. It is indicated that the measuring volume must be in the centre position, without rotation but titled 40°.

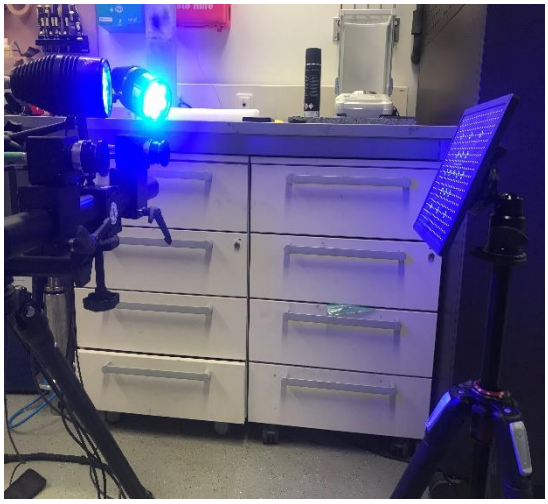

Figure 5.17. Representation of the fourth position during a real plate calibration.

In this step, the high of the cameras must be changed by means of the crank located in the calibration plate support or the one in the camera support. The calibration of the plate, allows the software to determine geometrical parameters, for example position and orientation of each camera based on the "snaps" taken.

When following the instructions, the exact distance that the panel is moved front or backwards is not important, due to the capacity of the software to determine whether it is too far or too close. The important issue during the movement is that the image does not get blurry so that the program can clearly detect the reference points of the calibration plate, as seen in Figure 5.15.

Due to the complexity of the operating system used by GOM, the software will always assist the user in case there is an error while the process is taking place. That means, if the plate is wrongly rotated, the cameras are not pointing to the correct spot, the image is too blurry, or the distance is too far or close, the software will always alert the user. For instance, in Figure 5.18 it can be seen how the software notifies an incorrect position of the cameras because the vertical reference point is lost. As a solution, the high of the cameras must be changed.

Figure 5.18. Example of an alert or advice during a calibration process. The position of the calibration object is invalid because the vertical position of the middle point is not correct.

After a thirteen-step calibration, the result is shown. If all the parameters are inside the range of optimal values, as in Figure 5.19, then the stage acquisition can start. Contrary, if the calibration is wrong and the deviation values are out of range, like in Figure 5.20, the calibration must be repeated. The complete calibration report or protocol can be downloaded as well, see Appendix A.

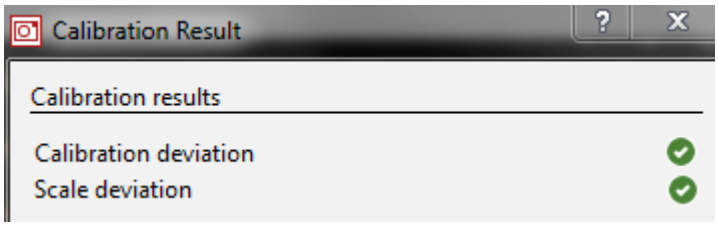

Figure 5.19. Example of a successful calibration result displayed by GOM Snap.

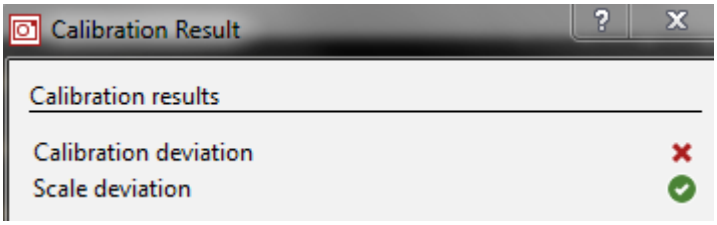

Figure 5.20. Example of an unsuccessful calibration result displayed by GOM Snap. Calibration deviation out of range.

5.1.2 Image Acquisition

The next step after a successful calibration is the image recording. The software allows the user to set up different frequencies for image acquisitions and the quantity of pictures desired. This process can be stopped whenever the user wants without losing the images captured. The time settle, in charge of making temperature increase and consequently increasing the brightness, should be the lowest possible or maximum 100 s. That will ensure a good picture without high brightness and with good contract of the black and white spots of the stochastic pattern. The following pictures (Figure 5.21, Figure 5.22 and Figure 5.23) exhibit the different views that the user observes when the brightness is changes.

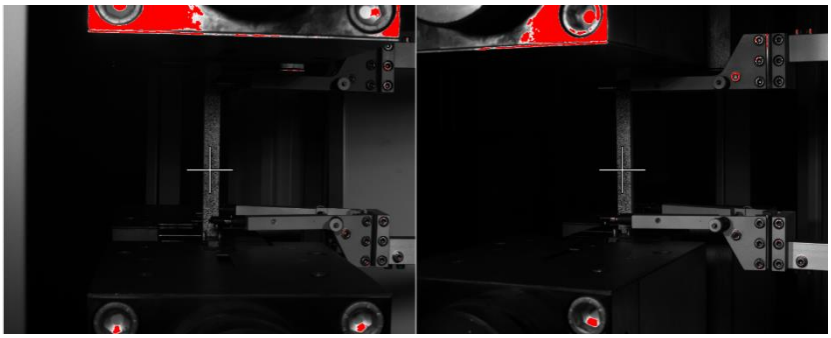

Figure 5.21. Example of a correct image acquisition (low light) for a tensile test.

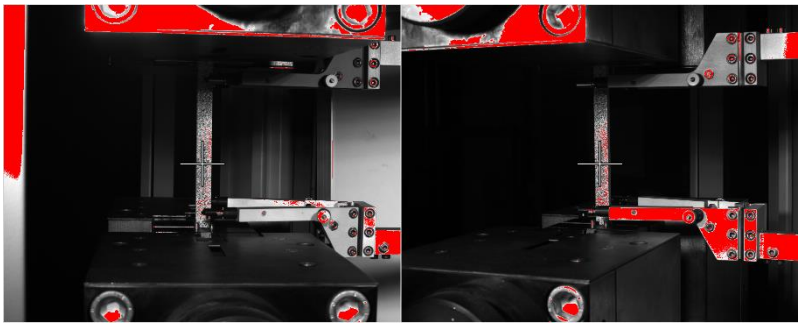

Figure 5.22. Example of an over lighting image acquisition for a tensile test.

Figure 5.23. Example of an over lighted specimen.

It is suggested that before the experiment takes place, a number of static pictures between 30 and 50 pictures are recorded to compute the noise of the image. Also, it is recommended to analyses these pictures to see if the software can clearly recognise the pattern and the surface can be computed.

In the stage acquisition it is also possible to manage the states to create subgroups of pictures and name them separately. This function is as well available in the further inspection software.

5.2 GOM Correlate Image Inspection

The evaluation of the 3D measuring date is made by means of GOM Correlate. The software allows the creation of elements, elements analysis and to create report pages. Below, all these functions are going to be explained in detail.

5.2.1 Element Creation

- **Point Component**

With reference point makers the computation is very simple. The function *Point Component* must be enabled, see Figure 5.24, and the operating system starts an automatic process of detection. Among the points detected, at least three must be chosen to constitute a *point component*, like Figure 5.25 shows.

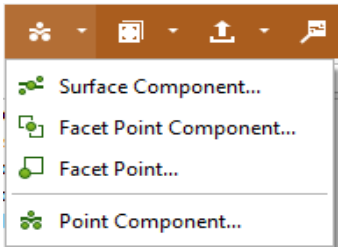

Figure 5.24. Available menu to enable the creation of different elements.

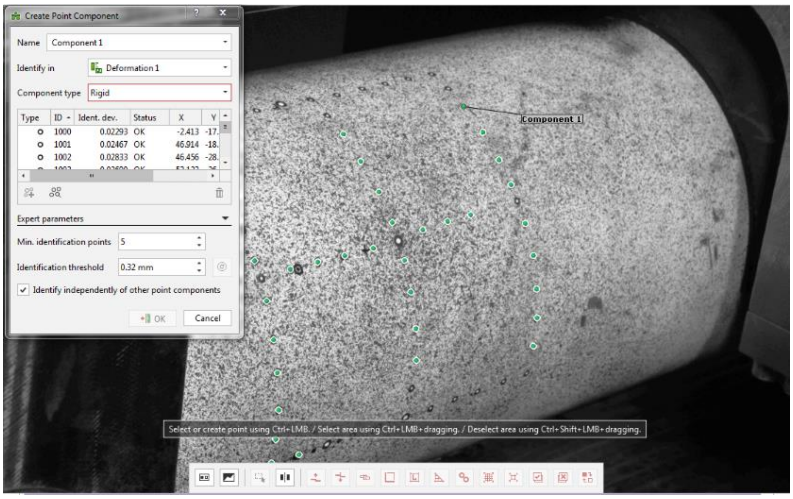

Figure 5.25. Example of point component detection in the 4PBT.

- **Surface Component**

For a stochastic pattern, the option *surface component* is chosen from the menu in Figure 5.24. The software will open a window, see Figure 35, in which several parameters of the surface can be configured to obtain the best surface. As observed in Figures 5.25 and 5.26, the configuration menus for creating a point component and a surface are different. The surface creation is based on the facet recognition in the stochastic pattern. Therefore, it is necessary to adjust some of the parameters that define the facets to generate a good surface for evaluation.

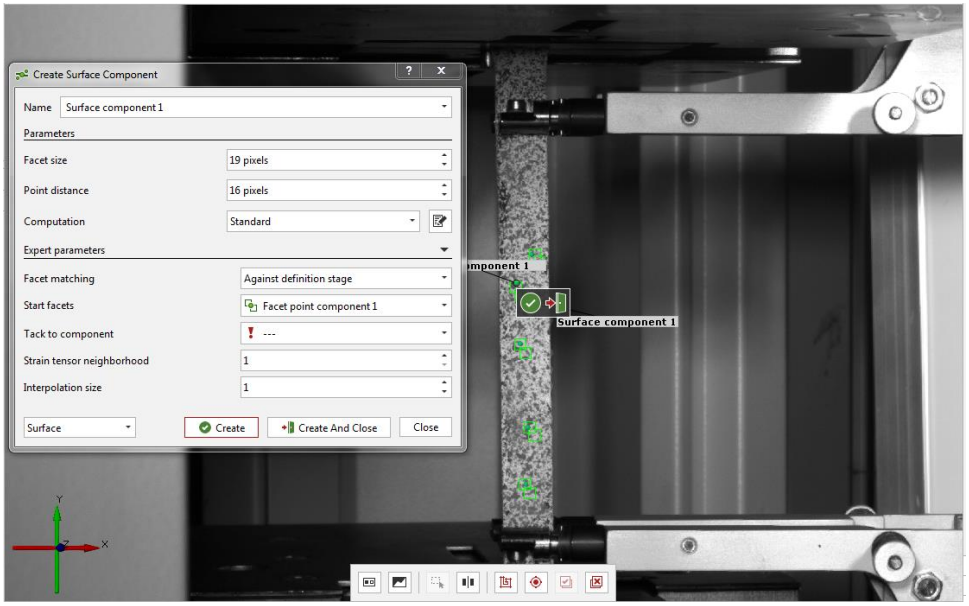

Figure 5.26. Surface component configuration menu. Example of the surface creation for the tensile test.

For the size and distance of the facets, the standard values given by GOM (19x19) are enough to ensure a good calculation. However, those values can be changed. The manuals recommend a facet size as small as possible, but large enough that the computation can be done. When the facet is larger than the default value, the acquisition of local effects within the facet is worse. Contrary, when the size of the facet is smaller than default, there is a better acquisition of the local effects within the facet. In addition, an overlap area between 20-50% must be settle for a useful computation and representation of the results [4].

The surface computation that will be used in most of the experiments is the standard computation, recommended by GOM. For the standard computation, high quality pattern is used and the intersection deviation of maximum 0,3 pixels is being used. The interpolation of the subpixels is bicubic. Sometimes it is not possible for the software to compute the surface using standard parameters and the setting need to be changed to "more points" computation. This setting is used when the quality of the facets is not the ideal but still can be detected with the GOM. The intersection requirements for this surface computation are lowered so that more facets can be computed when the computation is not possible even with this option, the calibration of the sensor needs to be repeated.

In chapter 6 the effect of these surfaces on the results computation is going to be explained.

Automatically, the surface computation is done using a random starting facet. Nonetheless, when the automatic search fails, it is possible to create a manual starting facet component, as can be seen in Figure 5.27. Therefore, as a proposition, is better to manually construct a starting facet component before creating the surface. This way of creating a facet component also can be helpful to know the quality of the points, which depend mostly on the pattern quality and the intersection deviation.

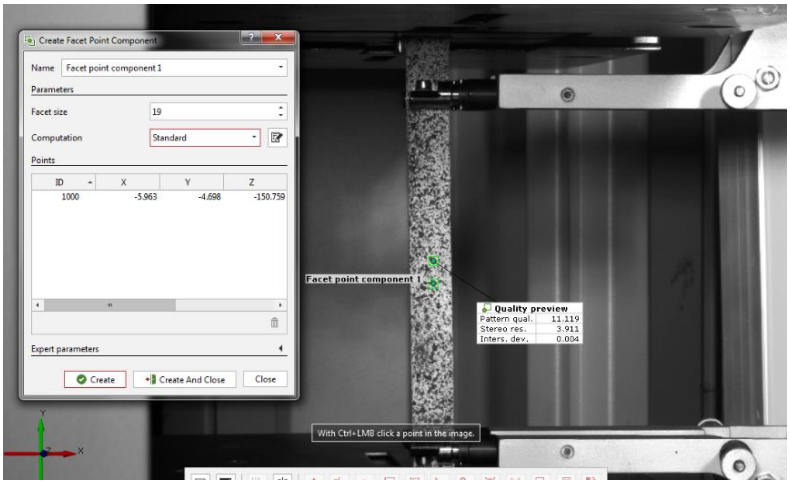

Figure 5.27. Example of the creation of a facet point component. The quality of the point is also observed.

When the surface is created, it is also possible to see the quality of the pattern applied and the intersection deviation.

The intersection deviation refers to the deviation in the computation of the 3D coordinate. As pointed out in section *3.2 Triangulation*, the system firsts find a 2D point in the left camera image and the same point in the right camera image. An observation ray results from each 2D point and the viewing direction of the camera. Ideally, the two observation rays intersect, and the software computes the 3D point from the intersection point of the observation ray. Since the observation rays of the camera are in the 3D space, they intersect only in one plane. A deviation can occur in the third plane. That is the described intersection deviation. The software computes the 3D point at the point of the minimum distance of each observation rate.

For the pattern quality display, as well as for the intersection deviation, the same legend of colours is being used. The green areas represent high quality of the pattern and low intersection deviation. That means that the gray values found in the left camera image can be identified well in the right camera image. The yellow areas determine a sufficient quality of the facets computed and larger intersection deviation. The identification of the gray values by the right camera is not optimal. Finally, red areas show bad quality pattern and larger intersection deviation. The software can badly identify the gray values found in the right camera image. Examples of this identification areas are illustrated in Figures 5.28 and 5.29.

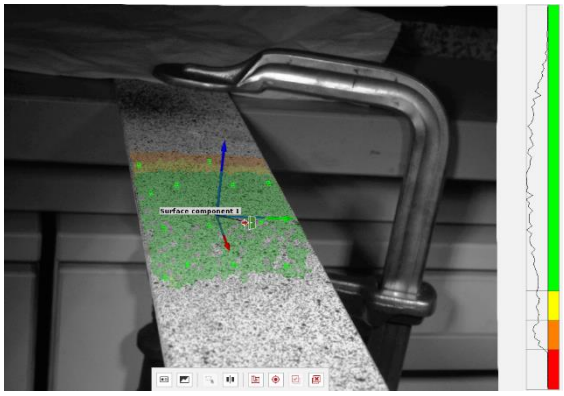

Figure 5.28. Example of the different pattern quality that can be found when creating a surface.

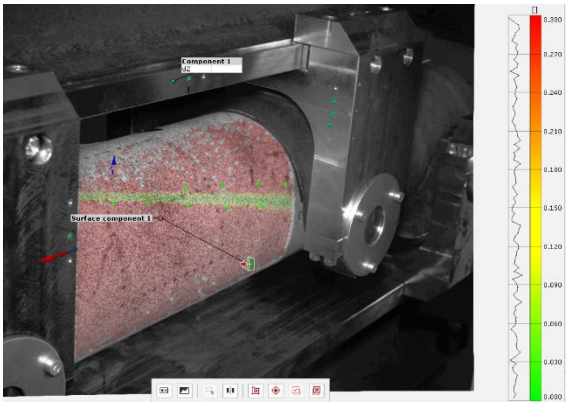

Figure 5.29. Example of the different intersection deviation areas that can be sound when creating a surface.

The figures above, represent examples of some of the trials made while trying to find the best setting and picture for the analysis of the measuring volumes. In the following chapter, for each different experimental test, the quality of the pattern and the intersection deviation is presented.

- **Alignment**

As mentioned in section 4.3 for calculating the strains the z axis must go in the direction of the material thickness.

Hence, the desired CS alignment must be adapted to the measuring volume. This process can be easily done by means of the 3-2-1 alignment option or the 3-points alignment, as indicated in Figure 5.30. The first option is based on the construction of 3 points that form a plane, 2 points that constitute a line and 1 point that generates the origin of the CS. The directions and axis orientations can be modified in the alignment parameters displayed windows, see Figure 5.31.
The second option is possible when a CAD file is imported. The user just needs to select three points of the original CAD design and match them with other three points on the surface created with GOM, like Figure 5.32 shows. The correlation between the original and the surface created points determines the position of the new CS.

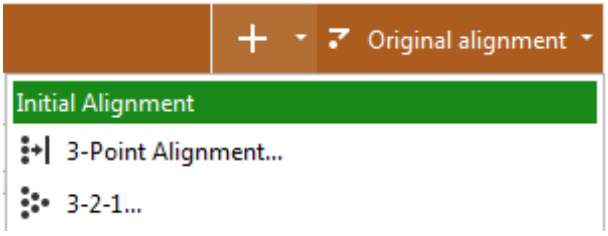

Figure 5.30. Available menu to enable the alignments.

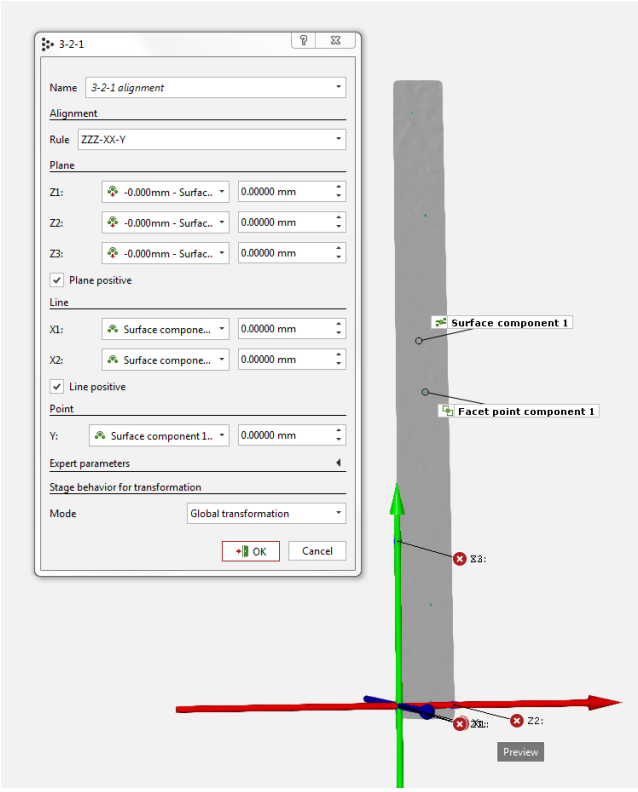

Figure 5.31. Example of a 3-2-1 alignment window for creating the correct coordinate system for one of the tensile test specimen.

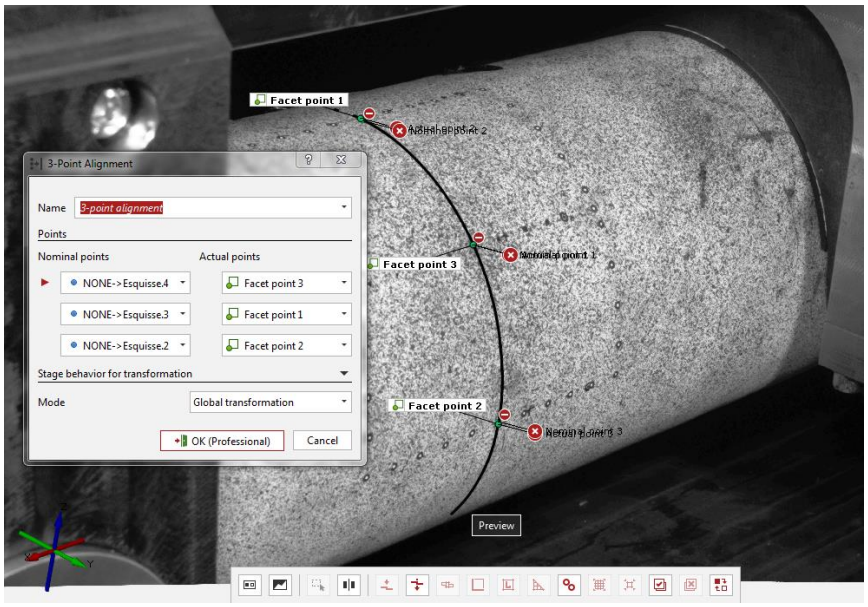

Figure 5.32. Example of the creation of a 3- Point alignment for the 4PBT.

5.2.2 Elements Analysis

In this step, the examination of the elements to obtain strains and displacements takes place. The surface analysis is represented with a coloured legend that shows the maximum and minimum values. If the exact value of a specific area or spot on the measuring object wants to be known, a deviation label must be placed. Additionally, surface points can be created on the surface to see all the results at one concrete point at the same time. For instance, when the displacements in the three directions want to be presented as well as the two directional strains, as in Figure 5.33.

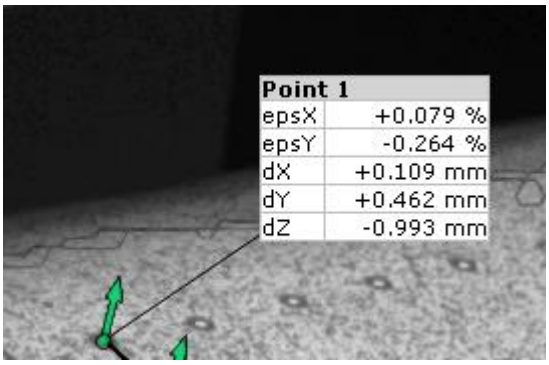

Figure 5.33. Inspection of a surface point in which is possible to see all the displacements and strains for that point at the same time.

The inspection can be done using different type of reference: a fixed value or a fixed reference stage. The last one must be settle manually in the stage manager, if not the reference stage is the first picture by default.

A part of the whole surface analysis, the program is also capable of creating sections, curves and lines which provide more detailed information of the section that wants to be analysed. All these different features are find out in the "construction" window, and the ones used are particularized on the coming chapter.

5.2.3 Report Page

To present and store the information obtained with the GOM Correlate, a report can be generated. Different structures can be created, combining graphs, pictures and videos with the corresponding data.

6. Evaluation Test Methods

In this following section, the theory detailed previously is applied in different tests, to assess the suitability of the GOM system. A simple cantilever test, a tensile test and a 3-Point Bending Test (3PBT) are done as trial test. The three of them present distinct setups which allow determining under which conditions the shows more satisfactory results.

6.1. Simple Cantilever Test

For this experiment, a simple cantilever beam is used made from aluminium and with the following dimensions 2x50x377 mm. The beam is clamped to the support table with a device that allows the limitation of the degrees of freedom of the beam. With 2 metallic pieces of 85 mm long and 50 mm width, with a weight of 0,58 kg each, a force of approximately 11,6 N (using gravity as 10 m/s^2) is applied.

- **GOM Configuration and Inspection**

According to the measuring volume that is recorded a calibration with the big calibration plate is performed. The measuring distance and the slider distance are 690 mm and 270 mm respectively.

Once the images are taken, the element inspection is done. A standard surface computation is done, and its pattern quality and intersection deviation are checked, as can be seen in Figure 6.1 and Figure 6.2 The resulting surface is the remaining between the metallic pieces and the built-in system.

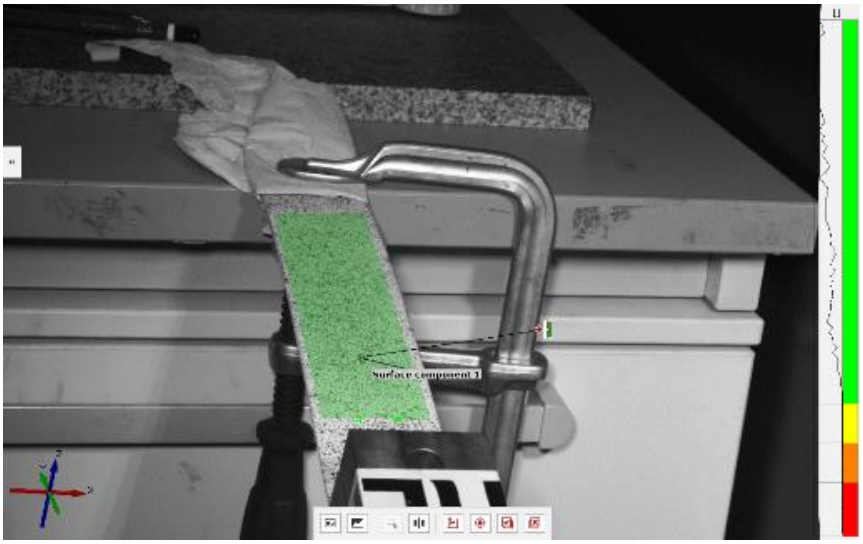

Figure 6.1 Representation of the pattern quality in the beam test evaluated.

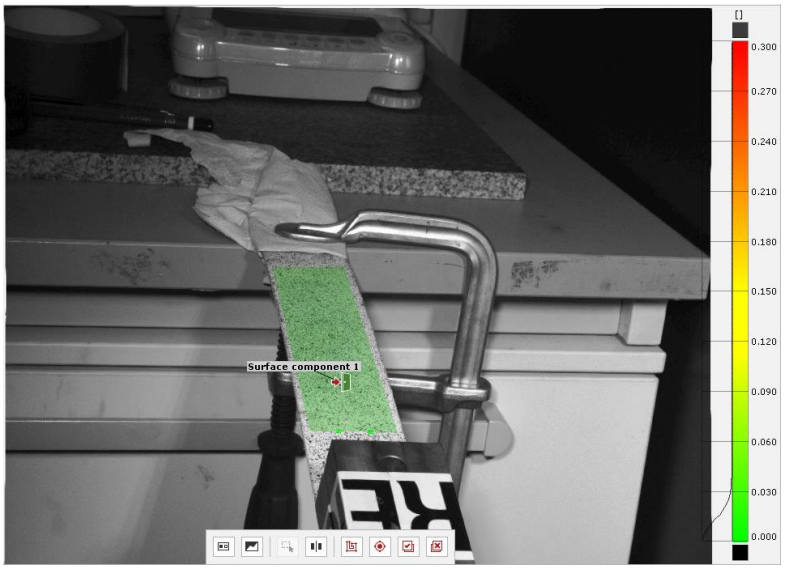

Figure 6.2. Representation of the intersection deviation in the beam test evaluated.

Before the actual element inspection, a correct alignment is created by means of the 3- 2-1 alignments, as Figure 46 shows.

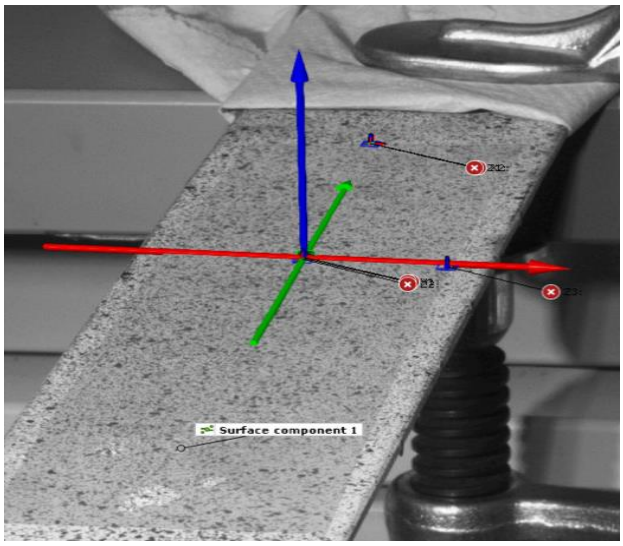

Figure 6.3. Correct alignment performed on the surface of the evaluated beam test.

- **Results Comparison**

As a first trial to evaluate the GOM strain computation, the cantilever beam has not been successful, because the strain value is too low to be computed by the software. That means that the obtained strain values with the GOM at the maximum deflection of the beam are altered by the noise and so, the obtained results cannot be exploitable. In Figure 6.4, the strain results for the examined area are between -0.1 % and 0.1 %. Inside this range, under 0.1 % of strain, the GOM system cannot display reliable results.

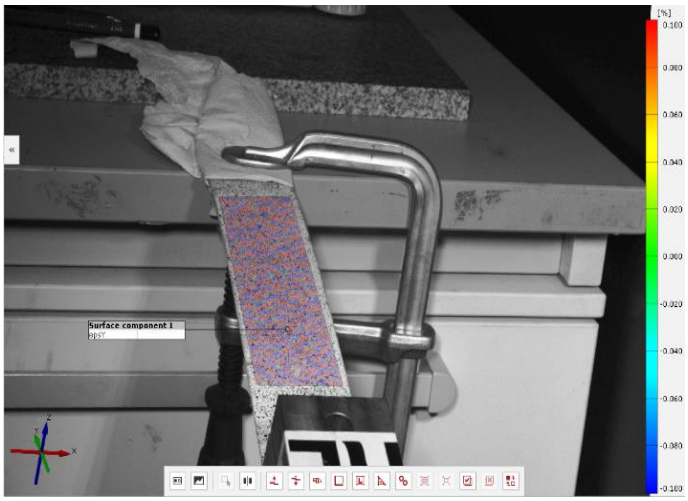

Figure 6.4. Representation of the strain in the y-direction of the analyzed cantilever beam.

Nevertheless, the experiment can be used to show the accuracy of the displacements computation. For that, the displacements in the Z axis are examined.

As can be seen in Figure 6.5, the analysed area is the one enclosed between the support and the force application. The length of that area is obtained using the option "distance" that can be found in the "construction" menu on the top part of the screen. The length of the surface is 163.9663 mm, as indicated in Figure 6.5.

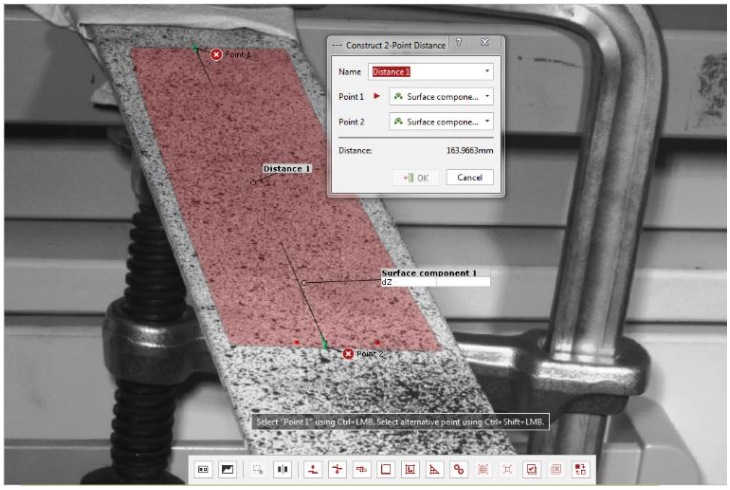

Figure 6.5. Distance representation of the analyzed area with the GOM system.

The results are expressed by the legend and, in addition, specific labels can be placed on the desired examination points to display the exact result, like Figure 6.6 exhibits. The maximum deflection found is 29.289 mm in the GOM results.

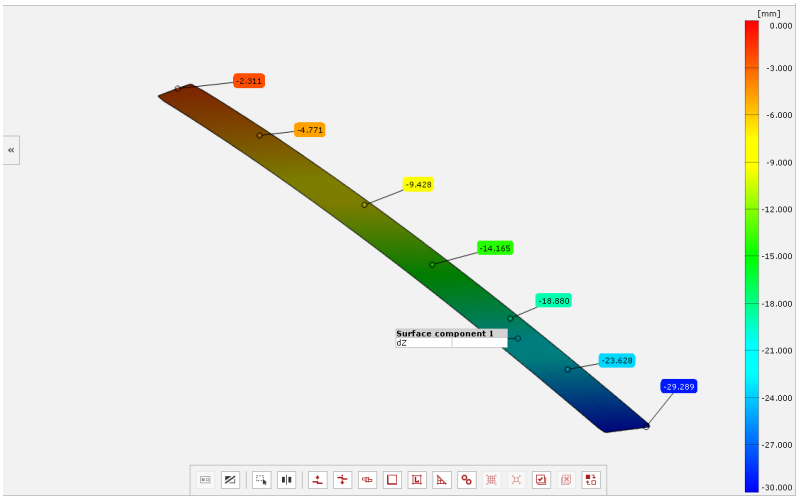

Figure 6.6. Representation of the displacements in the y-axis on the evaluated beam.

To compare the results obtained with GOM and validate them, a FEM simulation with SOLID WORKS of the same cantilever beam is used. In this representation, a beam of 350 mm is sketched because that is the real amount of beam that was free after fixing the support to the table. The results comparison must be done in the area just above the application of the force, that means, when the displacements have a value of 28.36 mm according to the FEM Simulation, see Figure 6.7.

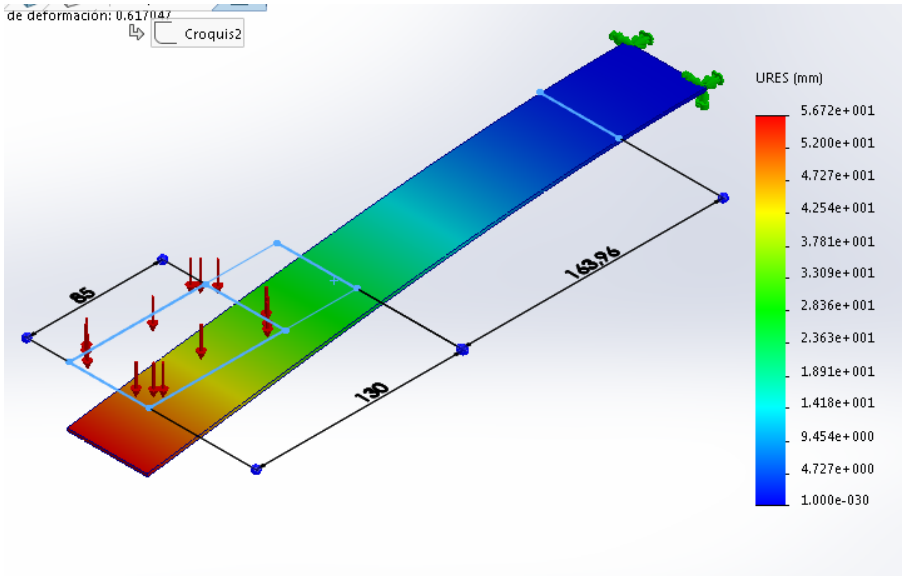

Figure 6.7. Displacements computed with SOLID WORKS.

The comparison shows a practically identical behaviour of the beam. The area that must be analysed is the one shown in the 163.96 mm in Figure 6.7. The maximum defection can be found at 130 mm of the free ping of the beam. This distance has been deduced using the pictures taken with GOM and the real beam, comparing the area where the surface is generated in GOM and the specimen. In that area, the maximum deflection is around 28.36 mm, see Figure 6.7. The difference between the values generated by GOM and solid work is around 0.929 mm.

The differences between the FEM values and the GOM results can be justified by the play of the experimental clamping system. In simulations, the clamping supports are very strict and ensure a total fixation of the element, whereas, in real experiments the play of the clamping device can interfere.

Finally, an analytical calculation can be done to match the results obtained before using the formula for point load applications [9] on one side fixed beams,

$$\delta = \frac{1}{6} \cdot \frac{P}{E \cdot I} \cdot l \cdot x^2 \cdot \left(3 - \frac{x}{l}\right), \tag{6.1}$$

where *P* is the force applied in the centre of the mass, l is the distance where the force is applied , x is the distance where the deflection is needed, *E* is the YOUNG Modulus of aluminium and *I* stands for the moment of inertia. The values of the distances are taken from the fixed point.

To clarify the distance and the conversion of the distrusted load into a punctual load, Figure 6.8. illustrates in a sketch the load application the beam, all the units are expressed in millimetres.

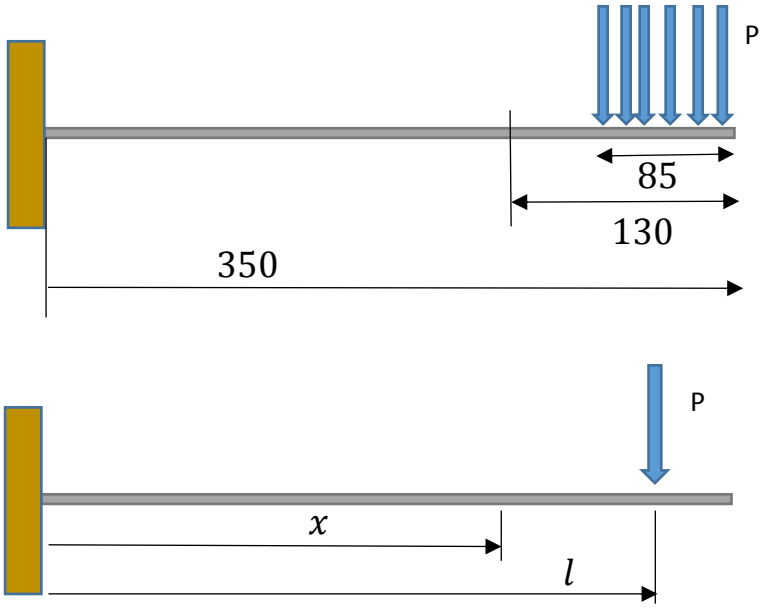

Figure 6.8. a) Schematic representation of the cantilever beam with the distributed load. b) Schematic representation of the cantilever beam with the punctual load.

The moment of inertia *I* is obtained with the formula

$$I = \frac{b^3 h}{12}, \tag{6.2}$$

in which *b* stands for the thickness of the beam, 2 mm, and *h* represents the width of it, 50 mm.
Replacing the parameters in equation 6.1 for the correct values, see equation 6.3, the analytical calculation of the deflection at the required point x=220 mm is:

$$\delta = \frac{1}{6} \cdot \frac{11.6}{70000 \cdot 33.3} \cdot \left(350 - \frac{85}{2}\right) \cdot (350 - 130)^2 \cdot \left(3 - \frac{(350-130)}{350-\frac{85}{2}}\right) = \frac{1}{6} \cdot \frac{11.6}{70000 \cdot 33.3} \cdot 307 \cdot 220^2 \cdot \left(3 - \frac{220}{307}\right) = 28.14\, mm \tag{6.2}$$

This result is very close to the one obtained with the FEM simulation and also close to the GOM result. The difference between the analytical al the GOM results can be justified as well by the possible play in the fixing support during the experiment.

6.2 Tensile Test

The goal of this test is to determine whether the results of the same test depend on the distance where the cameras are positioned.

- **Test execution**

The test is carried using the extensometers at the upper part of the universal test machine. To be able to record the process of elongation with the GOM system, the clamping grids are tilted 45°, as can be seen in Figure 6.9. The achieved view of the specimens with these configurations is the close to the optimal one, because the cameras are almost perfectly perpendicular to the specimen.

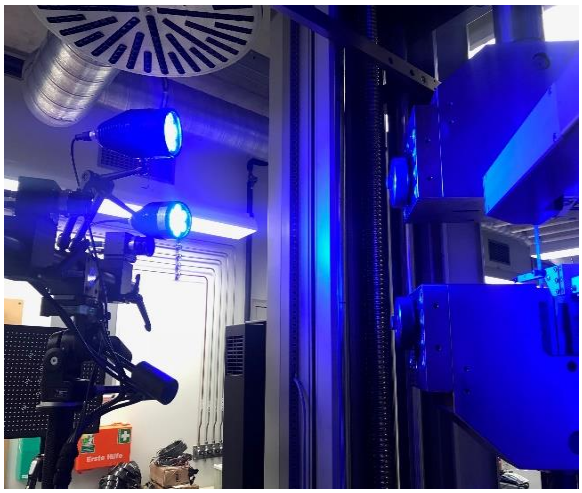

Figure 6.9. Picture of the whole set up of the whole set up where the clamping grids are rotated 45° and the cameras are located perpendicular to the specimen.

A total of 5 samples of Polyoxymethylene (POM) specimens are used to compare the results. The specimens are built following the norm ASTM D638-14. The specimens are sprayed with a stochastic pattern like Figure 6.10 shows.

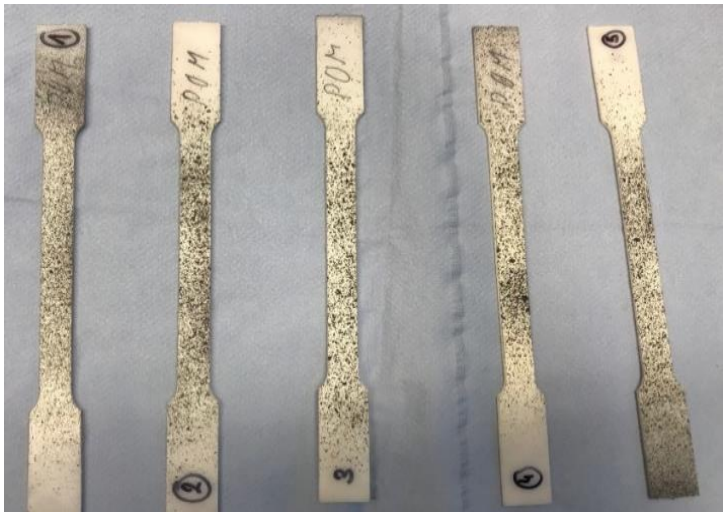

Figure 6.10. Stochastic pattern applied on the specimens

- **GOM Configuration**

The GOM system is positioned perpendicular to the specimen at the minimum distance that the infrastructure of the universal machine allows. Thus, the camera is positioned at 660 mm distance of the measuring object.
The calibration for this process is done using a camera distance of 660 mm and a slider distance of 256 mm. The slider distance is obtained by means of interpolation using the reference values of the GOM Manual [Page 19, Tab. 2. ARAMIS Adjustable Base 6M. [2]].
Once the slider and the camera distance are determined, the aperture and the focus need to be adjusted as well. The aperture used is the same recommended by the GOM Manuals for a big plate calibration at a 690 mm distance. Although the measuring distance is not the same, this aperture provides the best vision of the calibration plate ellipses and measuring object.
After the calibration process, the generated calibration report showed a successful calibration and a measuring depth of field of 260 mm. That means that it is possible to move the camera lenses to a maximum distance of 560 mm forwards and 810 mm backwards without changing the original calibration.

The standard surface computation was done, and the quality pattern and intersection deviation are checked. As seen in the upcoming pictures, Figure 6.11 and 6.12), both parameters are in the ideal state (all area is green coloured). Also, the alignment is adapted to the measuring volume, see Figure 6.13.

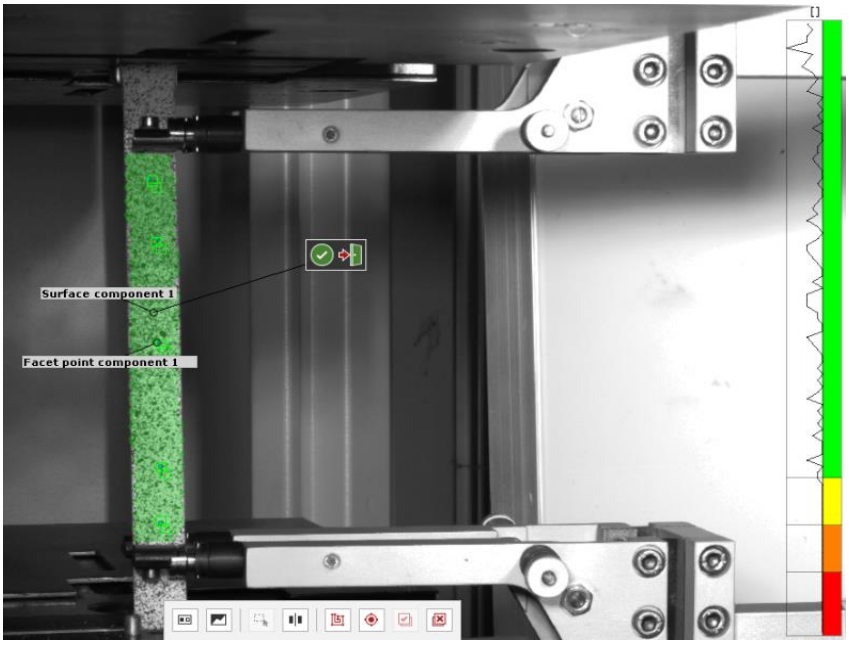

Figure 6.11. Representation of the pattern quality of one of an evaluated POM specimens.

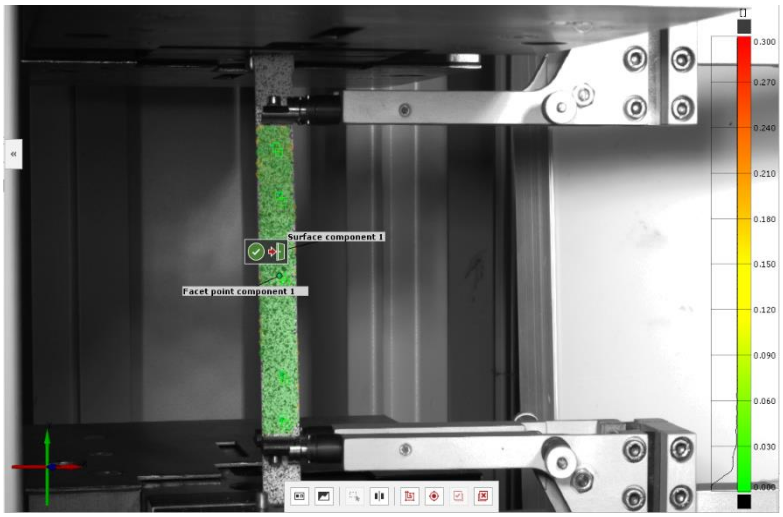

Figure 6.12. Representation of the intersection deviation of one evaluated POM specimen.

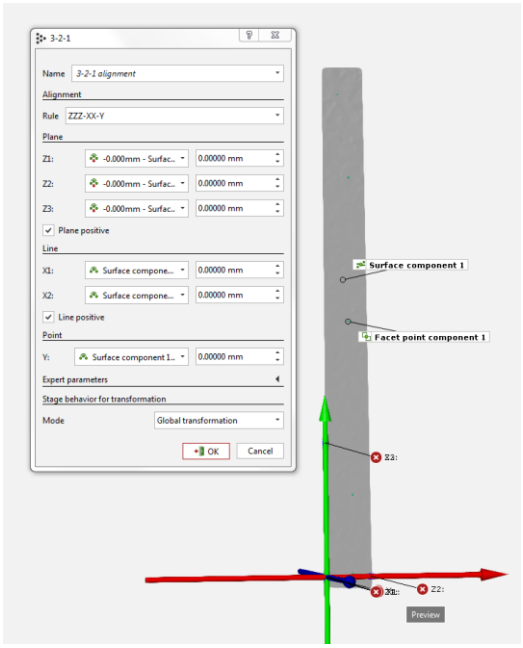

Figure 6.13. Correct alignment performed on the surface of an evaluated POM specimen.

- **Results computation**

After performing and recording the test for each POM specimen for the original calibration distance and the maximum far away position according to the DOF, the inspection with the GOM Correlate begins.
The strains in the y direction are being computed. The obtained results are documented in Table 2.

Table 2. Comparison of the GOM computed results between the two working distances.

Distance	**610 mm**	**810 mm**
Specimens	**Epsilon y (%)**	**Epsilon y (%)**
1	2,492	2,492
2	2,498	2,482
3	2,503	2,508
4	2,519	2,520
5	2,481	2,484
Average	2,498	2,497
Standard Deviation	0,014	0,016

The error is computed comparing the average result and the elongation specified in the universal testing machine. Table 3 indicates the results.

Table 3. Error comparison between the two working distances

	610mm	**810mm**
	Epsilon y	**Epsilon y**
Relative Error	0,004	0,003

In addition, the similar behaviour between the strain computation with GOM and with the universal test machine can be seen in Figure 6.14 and Figure 6.15.

The image acquisition with the GOM system stats at 0,5% strains to not obtain an elevated number of pictures that can be easily managed. Therefore, as shown in the next graphics, the comparison will be made between the 0,5% and 2,5% of strains.

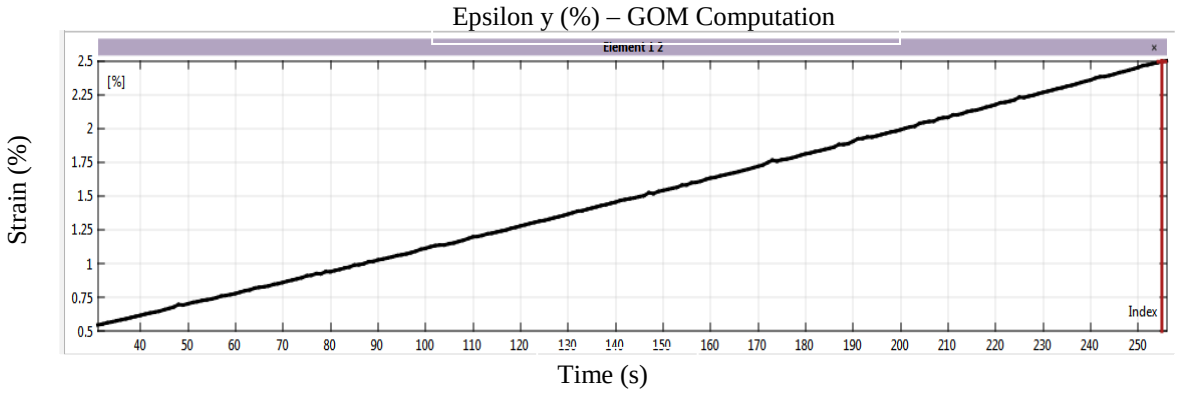

Figure 6.14. Diagram of the obtained epsilon y by means of the GOM Correlate. The time recoding starts at 30 seconds because before the load was applied, 30 pictures were taken to evaluate the noise.

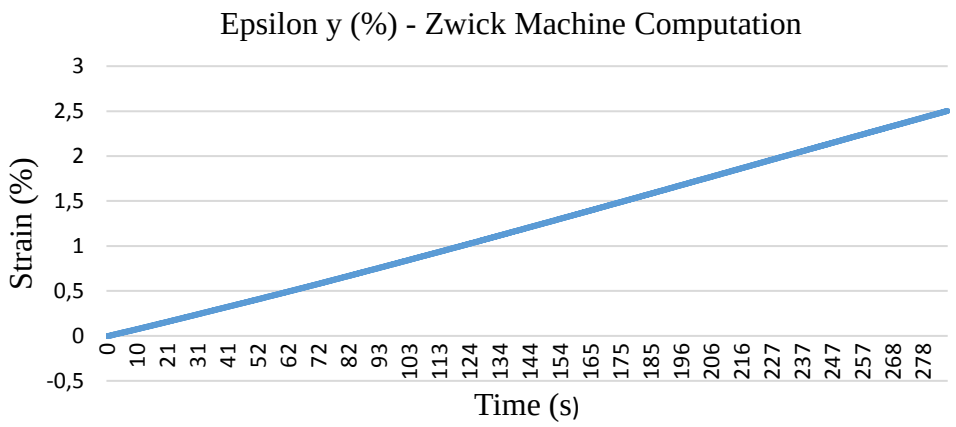

Figure 6.15. Diagram of the strain obtained with the ZWICK machine.

The main objective of these graphs is to show the linear behaviour of the strains recorded from the different sources. Is possible to see in Figure 6.14, how the diagram is not exactly straight and, although the line is clear, it is also possible to notice some small peaks, which are caused by the noise. The reached value, as mentioned, is in both cases 2,5 %.

6.3 3-Point Bending Test

The purpose of this experiment is to compare the results achieved with the GOM system with the ones provided with a unidirectional strain gage in the axial direction.

- **Test Execution**

For this test five POM specimens are being used. Their dimensions (150x115x53mm) have been defined according to DIN EN ISO178 [5] and considering that, there is enough space to place the strain gages. The specimens are sprayed with a stochastic pattern like Figure 6.16 shows.

Figure 6.16. Stochastic pattern applied on the POM specimens for the 3PBT.

The universal machine provides a 3-Point bending test (3PBT) equipment to execute tests in line with the international standardizations. The internal calculations of the universal machine are based in DIN EN ISO 14125 [10], as can be seen in Appendix B. However, there is no inconvenient because it uses the same computation procedure as DIN EN ISO 178. The flexural 3PBT apparatus is arranged in the clamping supports of the ZWICK machine, see Figure 6.17.

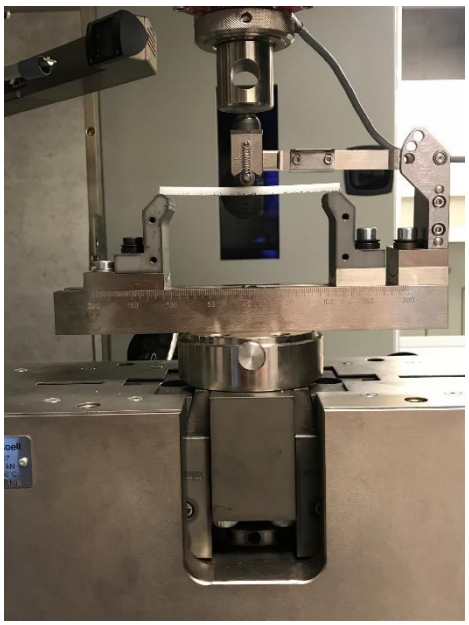

Figure 6.17. Setup of the 3PBT in the ZWICK machine.

As can be seen in Figure 6.17, the device consists of two parts: the supporting pins where the specimen lays and the top loading pin that applies the force into the specimen. The test consists on applying a force in the middle of the beam to measure different parameters, such as: flexural stress or flexural strain. In this case, the strain is the main evaluated parameter.
For the test, a maximum displacement needs to be configured in the ZWICK assistant and the dimensions of the measured object must be defined as well. In this case, a maximum displacement of 3 mm is determined. Once the displacement is specified the test begins. The traverse of the machine moves up until the supports pins achieve the fixed displacement.

The strain gage is in the middle of the beam where the force introduction takes place. More precisely it is placed as seen in Figure 6.18.

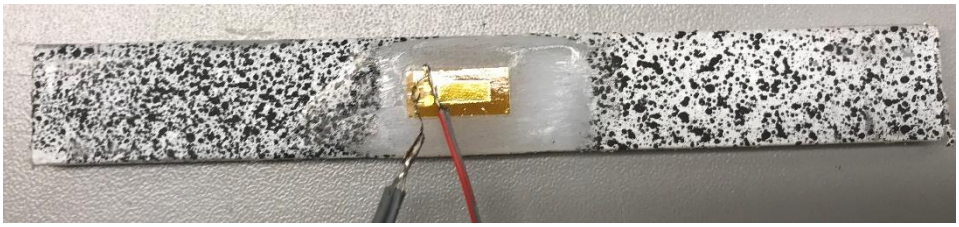

Figure 6.18. Placement of the unidirectional strain gage on the POM specimen.

The decision of placing a unidirectional strain gages is based on previous trials. In a previous test, a smaller bidirectional strain gage was placed and because of its reduced size and the configuration of the test, the welding between the wires and the strain broke. Therefore, a bigger sized strain is placed, although is just able to compute strains in the x-direction.

- **GOM Configuration**

For this procedure the emplacement of the GOM system is more complicated than the previous test because of the rotation angle that the cameras need to have for recording the required part. The distance used for the calibration is measured between the middle of the sensor and the measuring object and has a value of 360 mm. For that distance, a slider distance of 140 mm has been used.
A first trial of calibration with the cameras titled was conducted but the software did not allow its continuity because the image was too rotated. Therefore, the next calibrations are executed with the cameras pointing straight to the calibration plate.
After the successful calibration, the system is arranged to the correct position and the cameras are oriented to the measuring object trying to get the most possible perpendicular vision to the specimen surface, like can be observed in Figure 6.19. This change of camera position after a calibration leads to a high intersection deviation. The calibration parameters such as aperture and focus are not being changed, thus the image obtained are clear.

Figure 6.19. GOM setup for the image acquisition of the specimen.

However, as the orientation of the cameras is modified, the intersection deviation between both camera images acquired is high. As Figure 6.20 and Figure 6.21 show, the quality of the pattern is good, but the intersection deviation shows too high values. The consequences of this setup are discussed in the result computation.

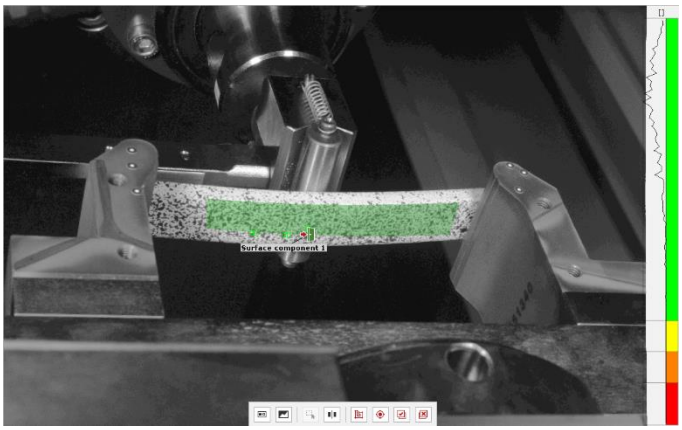

Figure 6.20. Representation of the pattern quality of an evaluated specimen for the 3PBT.

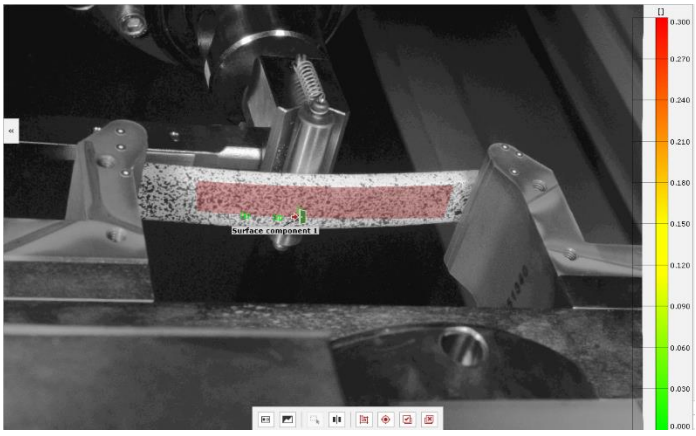

Figure 6.21. Representation of the intersection deviation of an evaluated specimen for the 3PBT.

Moreover, the alignment is performed using the 3-2-1 tool, as pointed out in Figure 6.22.

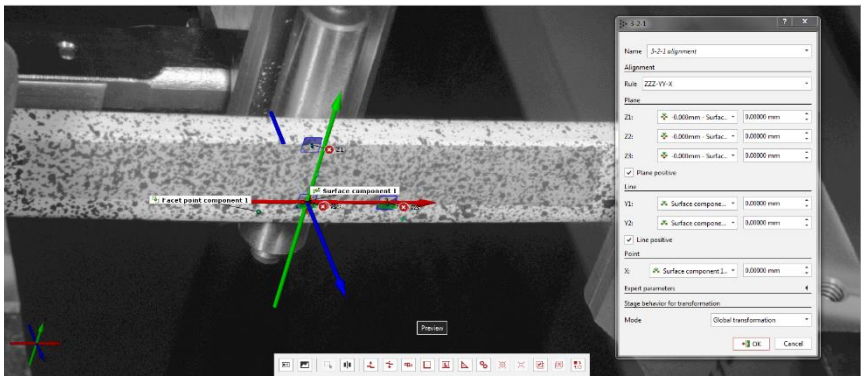

Figure 6.22. Correct alignment performed on the surface of an evaluated specimen for the 3PBT.

- **Results Computation**

  The unidirectional strain gage provides the results of the strains in the concrete spot where the device is arranged. As the object is deformed, the foil is also deformed, causing the electrical resistance to change. This change is related to the strain by the gage factor. The results of the strain calculation are represented in the ZWICK machine display as strains ($\mu m/m$). Those results need to be expressed in percentage, see Table 3, so that the comparison between both systems is possible.

Table 3. Results of the obtained values of the axial strain using strain gage.

	Strain Gage (%)
Specimen 1	0,795
Specimen 2	0,789
Specimen 3	0,793
Specimen 4	0,784
Average	**0,790**

On the other hand, the GOM Correlate allows the calculation of the strains and displacements on the entire surface to have an overall view of the deformation behaviour but also on other specific areas inside the surface component in which we can obtain the average value of strains. A 3D view of the surface generated and the strain value on the gage area can be observed in Figure 6.23.

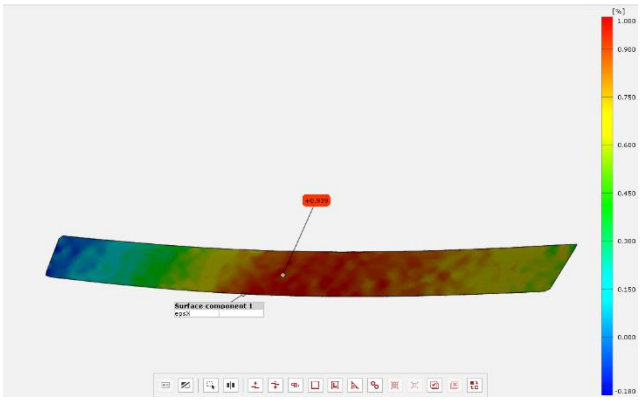

Figure 6.23. 3D view of the surface of a 3PBT specimen.
The average value on the strain gage area is 0,939 %.

This function is useful to compare the results exactly with the area where the strain gage is located. Table 4, summarizes the results of average mean of the axial strains in the area where the maximum strains are find and thus, where the strain gages are placed.

Table 4. Results of the axial strain computed with GOM.

	Strain (%)
Specimen 1	0,939
Specimen 2	0,952
Specimen 3	0,95
Specimen 4	0,948
Average	**0,947**
Standard Deviation	0,006

The absolute error between both measuring systems taking as a reference value the strain gage result is 0,16 %. The high differences between the computed results falls in the high values of intersection deviation registered.

Although the results are not satisfying, this experimental test can be used to determine that under difficult camera location configurations, that require a change of orientation after a proper calibration, the results can differ approximately 0,2% of the real or reference value.

In the following graphs, Figure 6.24 and Figure 6.25, the same linear behaviour can be observed in the strain computation for the two measuring devices.

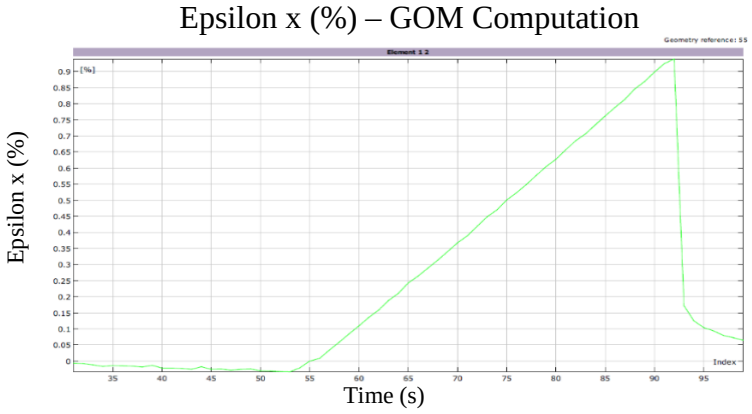

Figure 6.24. Graphical representation of the axial strain (epsilon x) computed with GOM.

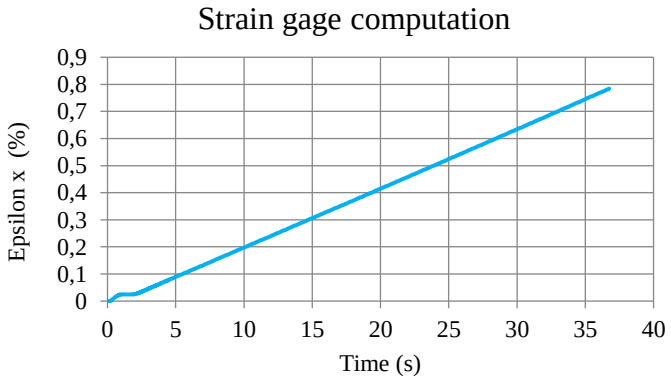

Figure 6.25. Graphical representation of the axial strain (epsilon x) computed with unidirectional strain gage.

The aim of this comparison is to show the linear behaviour of the strains recorded by both sources. It is also possible to see in Figure 6.24, that the preload was recorded and had an approximate duration of 55 s. Therefore, the starting point of the load can be set as second zero in the GOM graph and be directly compared to the one generated by the strain gage. For instance, by comparing the value of strain in second ten (65 s) in Figure 6.24 and the same second in Figure 6.25, there is almost a difference of 0.05% of strain between the values. This deviation is accumulated and increasing. For example, evaluating second 30 (second 85 in Figure 6.24), the deviation between the values is already 0.1%. Finally, it is observed that the final value is higher computed with the GOM that computed using strain gage.

Additionally, it can be seen in Figure 6.24, that the line behaviour is not exactly straight, that there are some small deviations from the total straight line. That is the effect of noise.

7. Evaluation on the 4-Point Bending Test

This section explains how the 4PBT is performed into a fibre-reinforced plastic composite tube, including the specimen preparation, the 4PBT structure assembly and the positioning of the GOM ARAMIS camera system. Afterwards, the results obtained are discussed and new solutions are proposed.

- **Test Execution**

A 4PBT is a testing method that provides the flexural data of a material. The test is made using two lower supports and two upper supports. Each of the upper supports introduces a load that will lead to the required bending moment.

The measured object is 1 m long and has an outer diameter of 133 mm. A schematic representation of how the supports and the forces are applied in the 4PBT is done in Figure 7.1. In this experimental case, the two upper supports induce a 10kN force, so 5kN each support, into the tube.

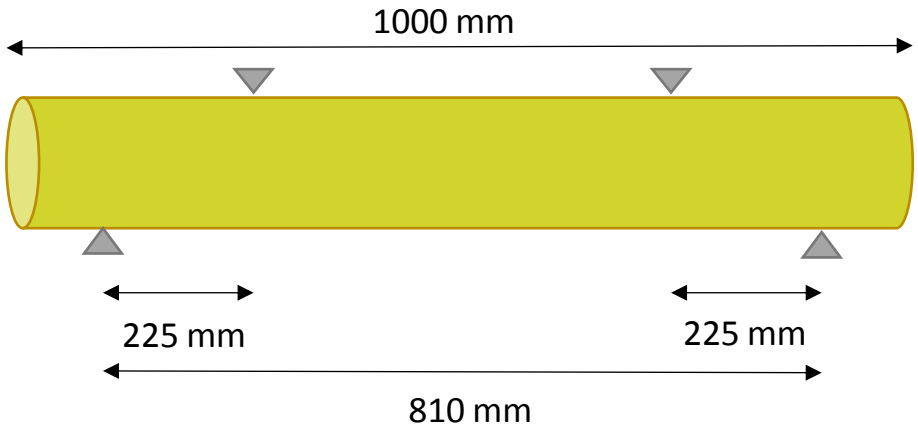

Figure 7.1. Schematic representation of the supports application on the 4PBT.

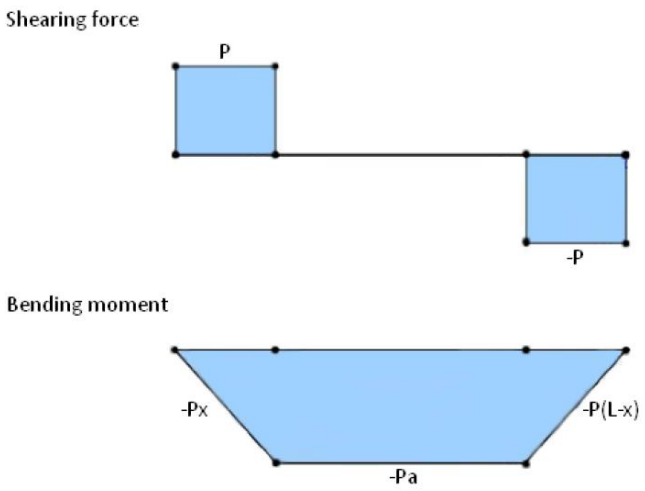

Figure 7.2. Shearing force and bending moment of a 4PBT [7].

One of the main interest of the test is the constant bending moment between the two upper supports with a value equal to $M = -Pa$ and no shear stress in that specific area as well, see Figure 7.2. Therefore, the middle area of the tube is the examined one.

The stochastic pattern was applied on the mentioned area. Also, point reference markers are added into this pattern to provide an easy recognition of the examined area when the images are taken, and the inspection of the elements is taking place. In addition, point reference markers can be used to display the displacement vectors in a graphical and clear way. The resulting area can be observed in Figure 7.3.

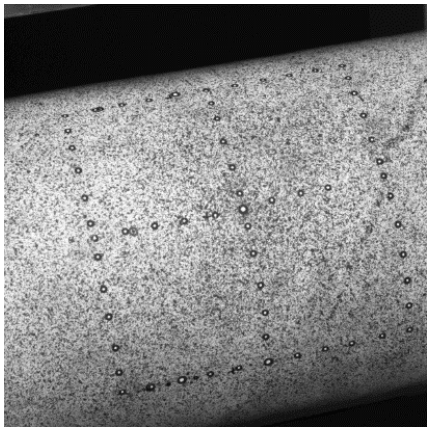

Figure 7.3. Combination of stochastic pattern and reference point markers on the tube.

Additionally, a bidirectional strain gage is located at the 45° of the not recorded site of the tube to have another validation of the GOM results.

The 4PBT system cannot be placed straight on the platform of the machine because if not it is impossible to record the deformations happening in the middle of the tub via GOM software. So, the whole structure should be titled and placed diagonally, see Figure 7.4.

- **GOM Configuration**

The decision of where the system should be positioned was since we needed the most cleared and spaced point of view of the tube. The best solution is placing the camera on the back side of the universal machine. Once the location is plausible, the orientation and high of the camera must be as well configured. The support of the camera is changed for a shorter one that also allow us to assembly another support that helps us to put the cameras closer to the specimen.

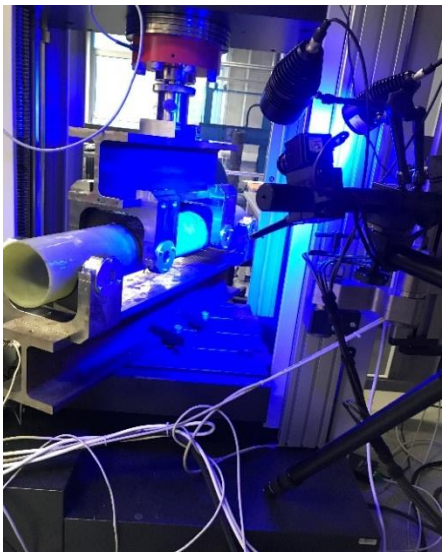

Figure 7.4. Setup of the GOM system for the image acquisition during the 4PBT.

The measuring distance used during the calibration is 690 mm with a slider distance of 270 mm. The successful calibration protocol displays a DOF of 260 mm. That technically means that the camera can be moved forward until a position of 580 mm without losing the calibration properties. The sensor is then moved into that range of distances until the perfect vision of the needed area is achieved.

It is necessary to highlight that there is a space limitation for the position of the cameras respect to the measured object. The accomplished location of the cameras is not the optimal, because the vision of the object is not exactly perpendicular. However, it will be shown in the following pictures, that the computation of the surface result is quite satisfying due to the good quality of the pattern applied and the low intersection deviation, see Figure 7.5 and Figure 7.6.

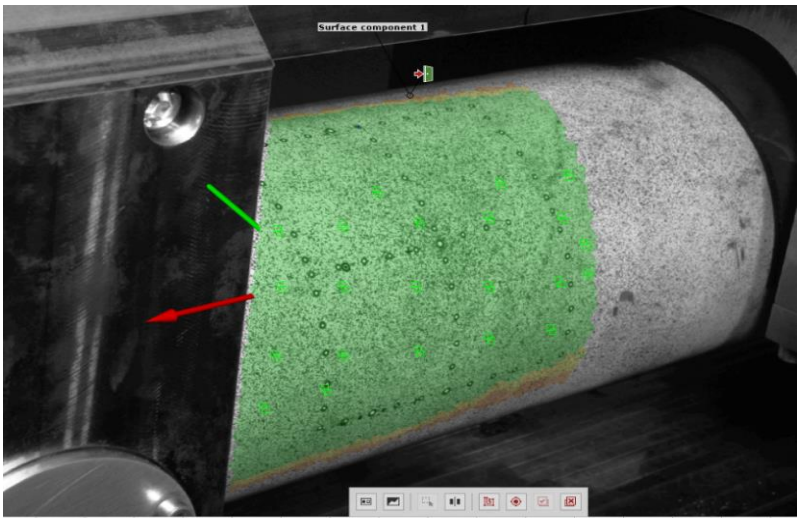

Figure 7.5. Representation of the pattern quality of the tube surface.

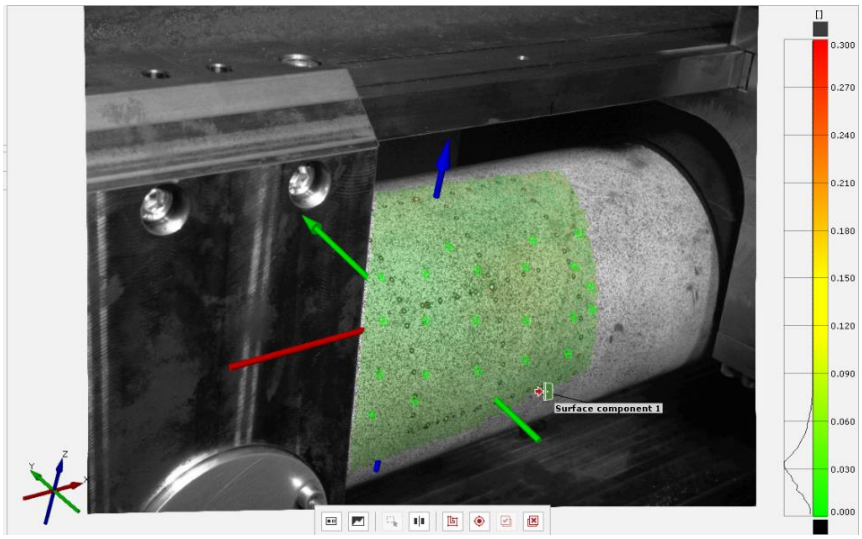

Figure 7.6. Representation of the intersection deviation on the evaluated surface.

In this case, the alignment has been made using the 3-point alignment tool explained in section 5.2. First, a tube of the same dimensions as the one used for the test is designed with a CAD software. In its surface three points are drawn in the 0°, 45° and 90° so that they can be aligned to the generated ones in GOM. Then, the file is imported into the GOM system. At the same time, on the resulting surface created with GOM, it is required to draw three points as well in the middle of the tube in the same angles mentioned before. Afterwards, the user must enable the 3-point alignment instrument. In the displayed menu, see Figure 7.7, the three points created in the CAD file are linked to the ones created with GOM. In Figure 7.8 is observed how the CAD tube is adjusted to the GOM model.

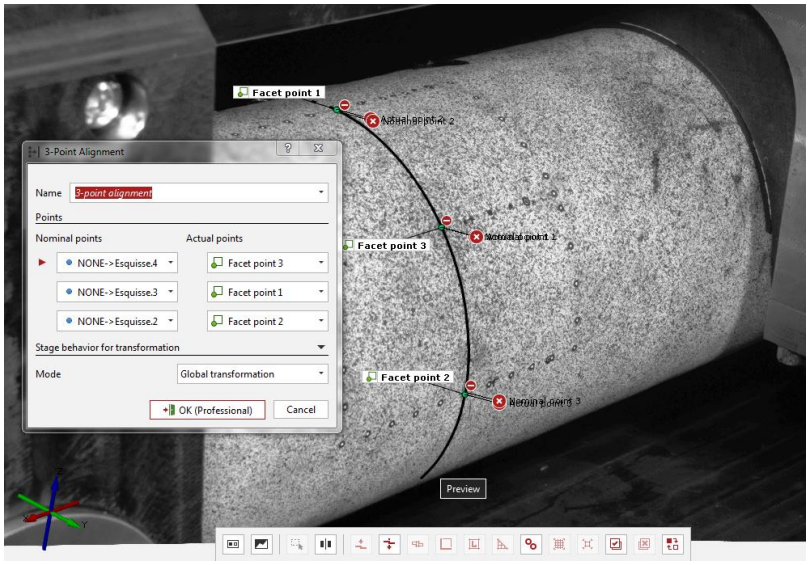

Figure 7.7. Example of how to perform a 3-point alignment in GOM Correlate.

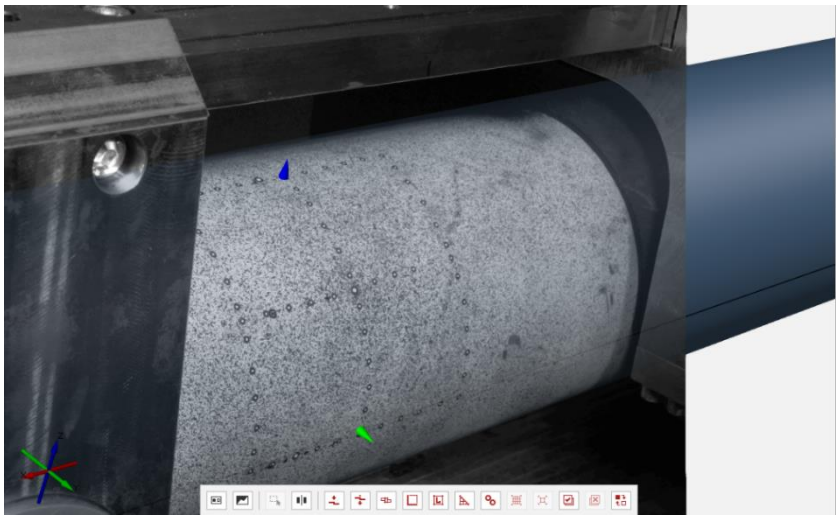

Figure 7.8. Correct alignment of a tube designed with CAD and the model represented with GOM.

- **Results Discussion**

In this test, the inspection with the GOM is made to compute the strains and the displacements in the Z and Y directions to analyse the deformation behaviour of the tube, more precisely the ovalization.
The strain computation has not been successful because of its small value. The strain accuracy is settled in 0,1%, and the experimental results obtained at the OTH Regensburg for the axial and circumferential strains by means of the strain gage are -0.032 % and 0.016 %, respectively [7]. These values are not big enough for the software to be differentiated from the ground noise of the optical measurement. Therefore, the obtained results for the strain computation via GOM are not valid and cannot be used as a reference for comparisons with other measuring devices. For instance, the results obtained from the bidirectional strain gage show coherent results in comparison to the numerical methods [Chart 8.1, Page 112, [7]].
As exhibit in Figure 7.9, the strain results can be cover up by the noise. The surface shows a constantly changing colour pattern that will provide distinct results for a specific area of examination in the same period. That means, that for the same spot observed when the image is static and there is no force applied, there strain results are very different from one stage to the other.

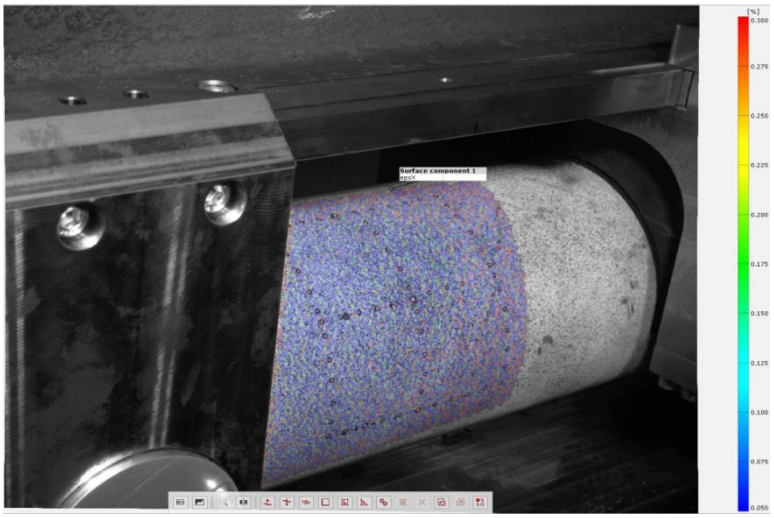

Figure 7.9. Noise representation on the x-strain of the evaluated area on a 4PBT.

The GOM system is thus used only to record, in this case, the displacements to inspect the deflection and the ovalization. The y-displacements and z-displacements have been computed, as presented in Figure 7.10 and 7.11.

As the following figures show, the displacements calculated with GOM in the middle of the tube show the highest value of Y displacements on the 0°.
Based on the theoretical studies of the ovalization of this specific tube, the top part of the tub (90°) should only be moving in the Z direction (downwards) and presenting the highest value of displacements in that direction. In addition, in the lateral side of the
tube (0°), the Z axis displacements should only represent the deflection. The deflection value obtained should be lower in the 0° position than in the 90° in which there are deflection and ovalization.

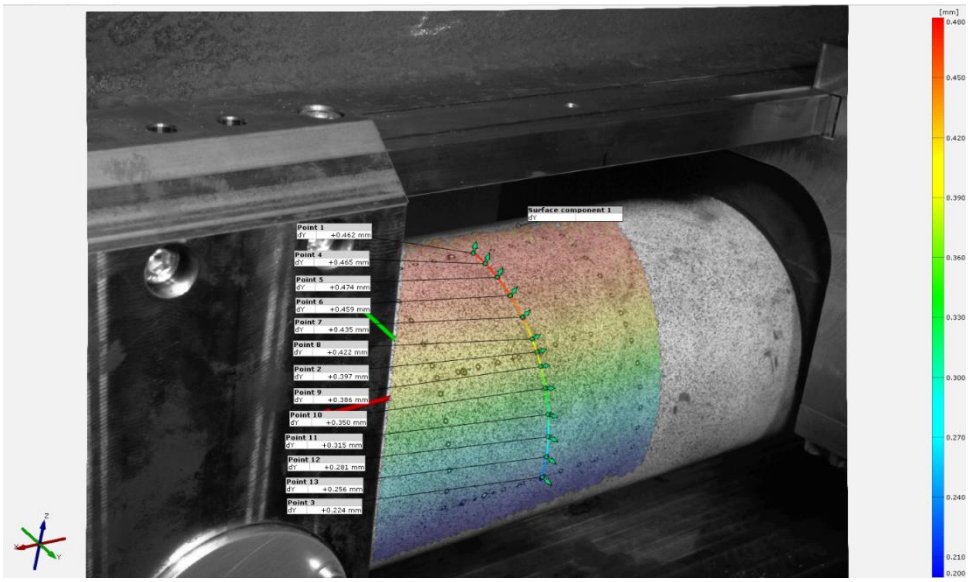

Figure 7.10. Displacements in the Y direction computed with GOM.

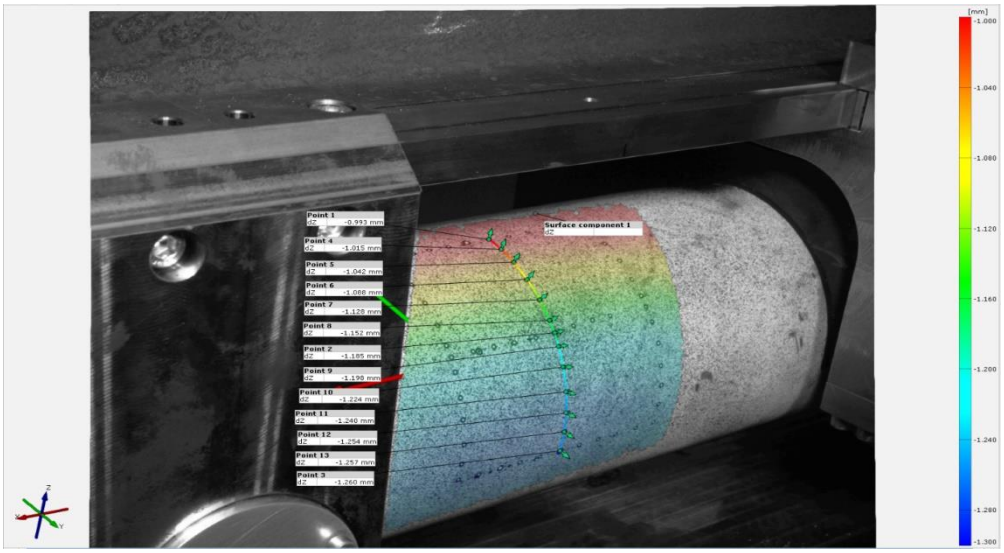

Figure 7.11. Displacements in the Z direction computed with GOM.

The explanation of this non-expected displacements recalls on the rotation of the tube while the force is applied. The 4PBT structure is designed with a 2mm think rubber between the tube and the real surface of the supports. With this rubber, the contact with the tube is bi-punctual and not linear as it should be. Because of this nonlinear contact, the tube tends to experiment a rotation that can be seen by eye.

To suppress the effect of the rotation, there are two possible adjustments that can be considered. On one side, an analytical approach can be developed using as assumption the theoretical behaviour of ovalization mentioned before. The y- displacement on the top of the tub are only due to rotation. The tube rotates around its axis, so that the displacement on the z-axis on the side of the tube (at 0º) is the same as the one of the y-axis on the top of the tube [7]. By this suppression and sing a sinus and cosinus rules for the projection, the net amount of deflection, see Figure 7.12, can be represented. The difference between the final deflection calculated at the top part and the one on the 0° allows the determination of the ovalization.

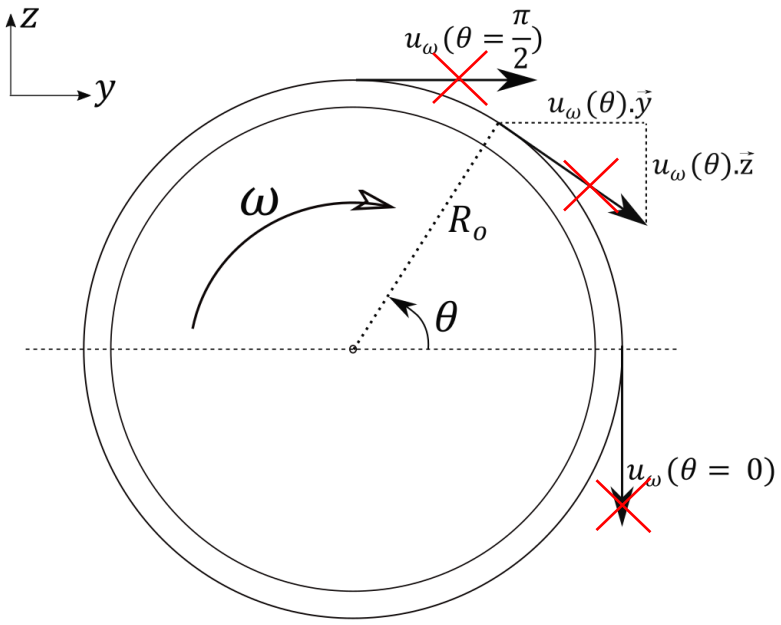

Figure 7.12. Assumption of the analytical suppression of the rotation [7].

Implying these assumption, the new values for the Y and Z displacements have been computed and represented graphically, comparing them to the undeformed state of the tube and the numerical results of deformation via ABAQUS simulation, exhibit in Figure 7.13.

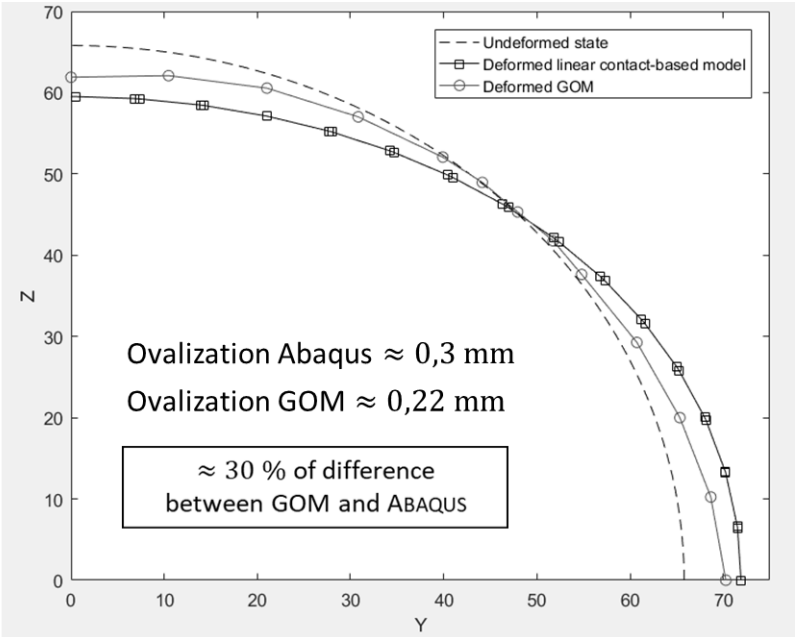

Figure 7.13. Comparison between the ovalization behaviour of the numerical analysis and the GOM processed results [7].

Even though the computed achieved results after this simplification show a coherent shape of the tube and ovalization behaviour, there is a maximum difference of 30 % between the values in the 90° and 0° computed with GOM and the ones accomplished via numerical method analysis. This analytical simplification leads to coherent, but not perfect results. Thus, another approach that can be experimentally proved must be applied.

For that reason, another thickness of the rubber must be used. As can be seen in the Figure 7.15, the thickness of the rubber influences the tube contact with the supports. On the figure below, the two different configurations are shown. On the left-hand side, the original 2 mm thickness rubber provides a bipunctual contact on the edges. On the right-hand side, a 1,5 mm thickness rubber provides a full contact between the tube and the bending test supports.

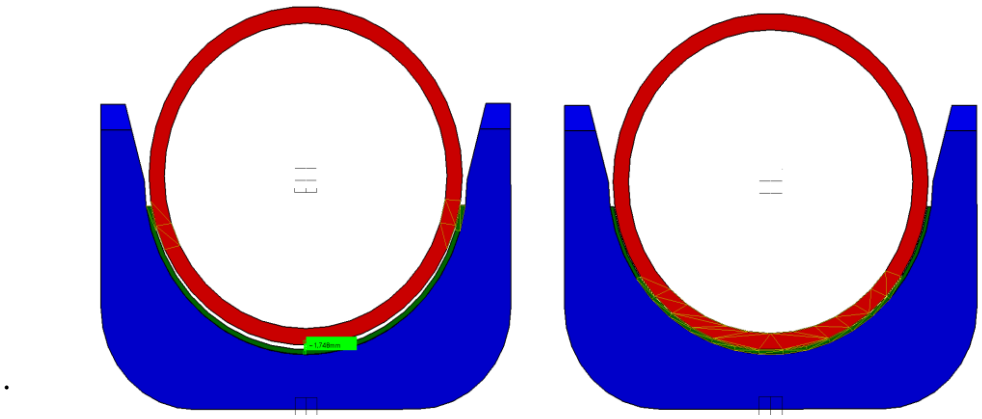

Figure 7.12. Comparison of the contact between the tube and the supports for a 2mm thickness rubber (left) and a new 1,5 mm thickness rubber (right) [7].

New test had been performed with the new rubber and no visible rotation has been appreciated with by eye. However, a further inspection with the GOM system must be performed to precisely determine that the rotation is supressed.

8. Conclusions and Further Perspectives

This thesis treated the determination of deformations and strains by means of the GOM ARAMIS Essential 6M Line. Although it has not been possible to obtain final values of the 4PBT carried out, other conclusions have been drawn from the more test performed that will be useful for further uses of the system. These dissertations recall not only result accuracy but also setup configuration and optimal use of the GOM ARAMIS.

In terms of accuracy and precisions, the capacity of the software to compute and display precise and reliable strain values is proved for strain values bigger than 0,1 %. Other smaller values are inside the possible noise values, which are implicit and inevitable in all DIC measurements. Although noise can be reduced with good quality pattern and low intersection deviation, it interferences and varies significantly the strain results when the values are under the mentioned amount.

The intersection deviation between both cameras must be the smallest to ensure accurate results. Therefore, it is recommended to use the ARAMIS system for test methods in which the cameras can be positioned the most perpendicular and straight way to the object, without any or few angles of rotation of the cameras. If the cameras need to be tilted, because of the setup of the experiment structure, it is suggested that a calibration with this camera angle is done. However, the software does not allow a calibration procedure if the angle is too high. Experimental test, such as the performed 3PBT, that more require camera rotation will not obtain satisfying and accurate results.

Another aspect tested and examined has been the distance. The DOF obtained after a successful calibration allows the movement of the cameras into that range of field, without losing the accuracy of the results, as seen in the performance of the tensile test.

Additionally, several improvement suggestions can be followed regarding the execution of the 4PBT and the GOM ARAMIS assembly. To suppress the rotation, a new test using the 1.5 mm rubber should be carried and recorded with the GOM ARAMIS system. Also, the application of higher forces on the tube may result into higher strain values that the image correlation system is able to measure precisely.

Finally, another approach discussed was the adaptation of a clamping device into the universal test machine that will allow a more direct and perpendicular view of the tub. However, the specifications of that new desired configuration should be deliberated with the GOM engineers to see if it's feasible to have a bigger angle between the cameras that the recommended, as represented in Figure 8.1.

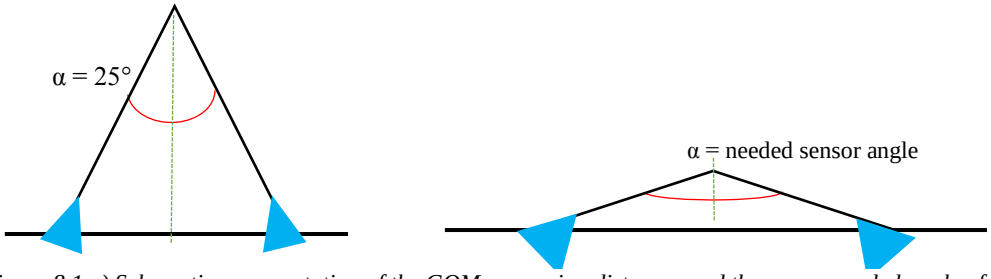

Figure 8.1 a) Schematic representation of the GOM measuring distances and the recommended angle of the cameras. b) Schematic representation of the required future measuring distance and the needed sensor angle for this new configuration.

References

[1] N.N.: *GOM Acquisition Basic.* Aramis Manual GOM. GOM GmbH, Braunschweig, 2016.

[2] N.N.: *GOM Adjustable Base. User manual Hardware.* Aramis Manual GOM. GOM GmbH, Braunschweig, 2016.

[3] N.N.: *GOM Testing. Digital Image Correlation and Strain Computation Basics.* Aramis Manual GOM. GOM GmbH, Braunschweig, 2016.

[4] N.N.: *GOM Inspection Basics. 3D Testing.* Aramis Manual GOM. GOM GmbH, Braunschweig, 2016.

[5] N.N.: *DIN EN ISO 178:2010: E Plastics – Deformation of Flexural Properties*. European Standard Institut, Brusels, 2003.

[6] N.N.: *ASTM 638-14. Standard test Method for Tensile Properties of plastics.* American Society for Testing and Materials, West Conshohocker PA, 2014

[7] VAUGE, A.; EHRLICH,I.: *Analytical Description of the Ovalization and Testing of Fiber-Reinforced Tubes in a 4-Point Bending Test.* Ostbayerische Technische Hochschule Regensburg, Regensburg 2018.

[8] Schmidt, K.J.: *Festigkeitslehre. Skriptum zur Vorlesung Technische Mechanik 2.* December, 2009.

[9] N.N.: *Photogrammetric Methods for 3D Measuring Technology*. Aramis for Education. GOM GmbH, 2016.

[10] DIN EN ISO 1425; *Fiber-Reinforced Plastic Composites – Determination of flexural properties.* Deutsches Institut für Normung e.V, Berlin, 1998.

Appendices

A Calibration Protocols

A.1 Calibration protocol for the cantilever beam test

Current Calibration Info

General	
Calibration date	Tue Jul 3 19:06:27 2018
Calibrated sensor	
Sensor name	ARAMIS Adjustable Base
Measuring volume	Adjustable measuring volume
Camera support	Adjustable base 500
Working distance	690 mm
Camera angle	25°
Camera distance	270 mm
Serial number	no identifier
Calibration object	
Object type	Panel (coded)
Name	Kalibrierplatte 350x280
Calibration scale	Distance 1: 312.000 mm
	Distance 2: 312.000 mm
Certification temperature	20.0 °C
Expansion coefficient	$22.90 \times 10^{-6}\ K^{-1}$
Calibration temperature	25.0 °C
Calibration settings	
Camera lenses	24.00 mm
Snap mode	Single snap
Ellipse quality	0.4
Calibration Result	
Calibration deviation	0.018 Pixels
Calibration deviation (check)	OK (limit value: 0.050 Pixels)
Scale deviation	0.024 mm
Scale deviation (check)	OK (limit value: 0.031 mm)
Camera angle	25.6°
Height variance	344 mm
Measuring volume	325 / 270 / 270 mm

A.2 Calibration protocol for the tensile test

Current Calibration Info

General

Calibration date	Mon Jul 9 12:00:47 2018

Calibrated sensor

Sensor name	ARAMIS Adjustable Base
Measuring volume	Adjustable measuring volume
Camera support	Adjustable base 500
Working distance	660 mm
Camera angle	25°
Camera distance	256 mm
Serial number	no identifier

Calibration object

Object type	Panel (coded)
Name	Kalibrierplatte 350x280
Calibration scale	Distance 1: 312.000 mm
	Distance 2: 312.000 mm
Certification temperature	20.0 °C
Expansion coefficient	$22.90 \times 10^{-6}\ K^{-1}$
Calibration temperature	25.0 °C

Calibration settings

Camera lenses	24.00 mm
Snap mode	Single snap
Ellipse quality	0.4

Calibration Result

Calibration deviation	0.017 Pixels
Calibration deviation (check)	OK (limit value: 0.050 Pixels)
Scale deviation	0.025 mm
Scale deviation (check)	OK (limit value: 0.031 mm)
Camera angle	25.2°
Height variance	215 mm
Measuring volume	320 / 260 / 260 mm

A.3 Calibration protocol for the 3PBT

Current Calibration Info

General

Calibration date	Thu Jul 19 17:12:48 2018

Calibrated sensor

Sensor name	ARAMIS Adjustable Base
Measuring volume	Adjustable measuring volume
Camera support	Adjustable base 500
Working distance	360 mm
Camera angle	25°
Camera distance	140 mm
Serial number	no identifier

Calibration object

Object type	Panel (coded)
Name	Kalibrierplatte 175x140
Calibration scale	Distance 1: 140.000 mm
	Distance 2: 140.000 mm
Certification temperature	20.0 °C
Expansion coefficient	$4.00 \times 10^{-6}\ K^{-1}$
Calibration temperature	25.0 °C

Calibration settings

Camera lenses	24.00 mm
Snap mode	Single snap
Ellipse quality	0.4

Calibration Result

Calibration deviation	0.029 Pixels
Calibration deviation (check)	OK (limit value: 0.050 Pixels)
Scale deviation	0.003 mm
Scale deviation (check)	OK (limit value: 0.014 mm)
Camera angle	26.8°
Height variance	136 mm
Measuring volume	170 / 140 / 125 mm

A.4 Calibration protocol for the 4PBT

Current Calibration Info

General

Calibration date	Wed Jun 13 09:30:28 2018

Calibrated sensor

Sensor name	ARAMIS Adjustable Base
Measuring volume	Adjustable measuring volume
Camera support	Adjustable base 500
Working distance	690 mm
Camera angle	25°
Camera distance	270 mm
Serial number	no identifier

Calibration object

Object type	Panel (coded)
Name	Kalibrierplatte 350x280
Calibration scale	Distance 1: 312.000 mm
	Distance 2: 312.000 mm
Certification temperature	20.0 °C
Expansion coefficient	$22.90 \times 10^{-6}\ K^{-1}$
Calibration temperature	25.0 °C

Calibration settings

Camera lenses	24.00 mm
Snap mode	Single snap
Ellipse quality	0.4

Calibration Result

Calibration deviation	0.025 Pixels
Calibration deviation (check)	OK (limit value: 0.050 Pixels)
Scale deviation	0.023 mm
Scale deviation (check)	OK (limit value: 0.031 mm)
Camera angle	23.8°
Height variance	211 mm
Measuring volume	350 / 290 / 290 mm

B Zwick Protocols

B.1 Zwick protocol for the tensile test

Zwick / Roell

10.08.18

Prüfprotokoll

Kunde	:	Probentyp	:
Auftrags-Nr.	:	Vorbehandlung	:
Prüfnorm	:	Prüfer	:
Art und Bezeichnung	:	Bemerkung	:
Werkstoff	:	Maschinendaten	:
Probenentnahme	:		

Vorkraft	:	0,1	MPa
Prüfgeschwindigkeit	:	1	mm/min

Prüfergebnisse:

	σ_M	ε_M	h	b	A0
Nr	MPa	%	mm	mm	mm²
9	3,56	2,5	2,5	125	312,50
12	3,61	2,5	2,5	125	312,50
31	3,71	2,5	2,5	125	312,50
33	3,69	2,5	2,5	125	312,50
35	3,61	2,5	2,5	125	312,50
39	3,67	2,5	2,5	125	312,50
43	3,61	2,5	2,5	125	312,50
44	3,60	2,5	2,5	125	312,50
46	3,69	2,5	2,5	125	312,50
48	3,69	2,5	2,5	125	312,50

Seriengrafik:

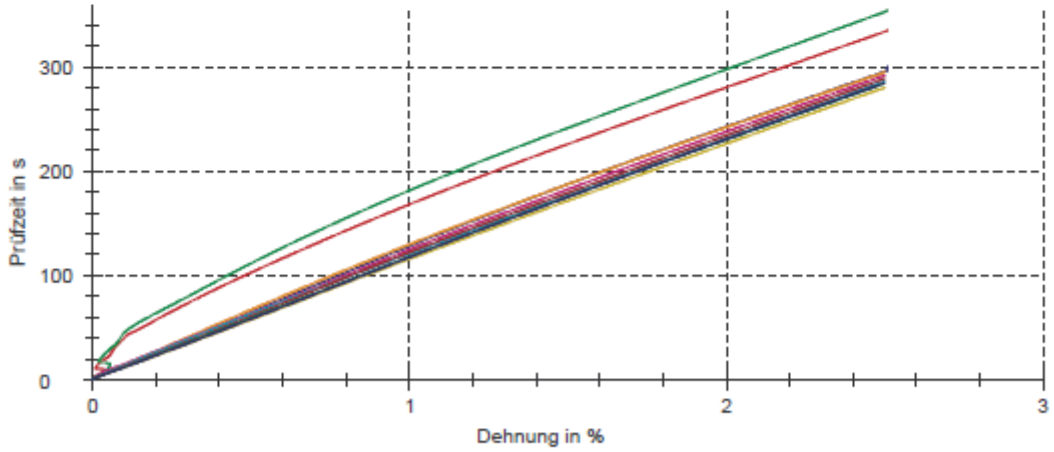

Zwick / Roell

10.08.18

Statistik:

Serie	σ_M	ε_M	h	b	A_0
n = 10	MPa	%	mm	mm	mm²
$\bar{x}$	3,65	2,5	2,5	125	312,50
s	0,0500	0,0	0,000	0,000	0,00
v [%]	1,37	0,14	0,00	0,00	0,00

B.2 Zwick protocol for the 3PBT – GOM measurements

Zwick / Roell

11.09.18

Prüfprotokoll

Kunde	:	OTH Regensburg	Probentyp	:	
Auftrags-Nr.	:		Vorbehandlung	:	
Prüfnorm	:	DIN EN ISO 14125	Prüfer	:	Andreas Kastenmeier/Max Faber
Art und Bezeichnung	:	FW2-3-Punktbiegeversuche	Bemerkung	:	
Werkstoff	:	FW2 CFK	Maschinendaten	:	
Probenentnahme	:				

Prüfung	:	Verfahren A
Vorkraft	:	1 N
Prüfgeschwindigkeit	:	5 mm/min

Prüfergebnisse:

Nr	Probenkennung	Datum/Uhrzeit	σ_f' MPa	σ_f'' MPa	E_f GPa	σ_{fC} MPa	σ_{fM} MPa	ε_M %	L mm	h mm
2	FW2-B001_119_V4	19.07.2018 18:38:56	0,911	1,406	1,00	-	-	-	106	5,3
5	FW2-B001_119_V4	19.07.2018 18:48:05	0,882	1,378	1,00	-	-	-	106	5,3
6	FW2-B001_119_V4	19.07.2018 18:53:17	0,824	1,267	0,896	-	-	-	106	5,3
9	FW2-B001_119_V4	19.07.2018 19:00:30	0,867	1,351	0,962	-	-	-	106	5,3
10	FW2-B001_119_V4	19.07.2018 19:03:05	0,864	1,288	0,869	-	-	-	106	5,3

Nr	b mm
2	15,2
5	15,2
6	15,2
9	15,2
10	15,2

Seriengrafik:

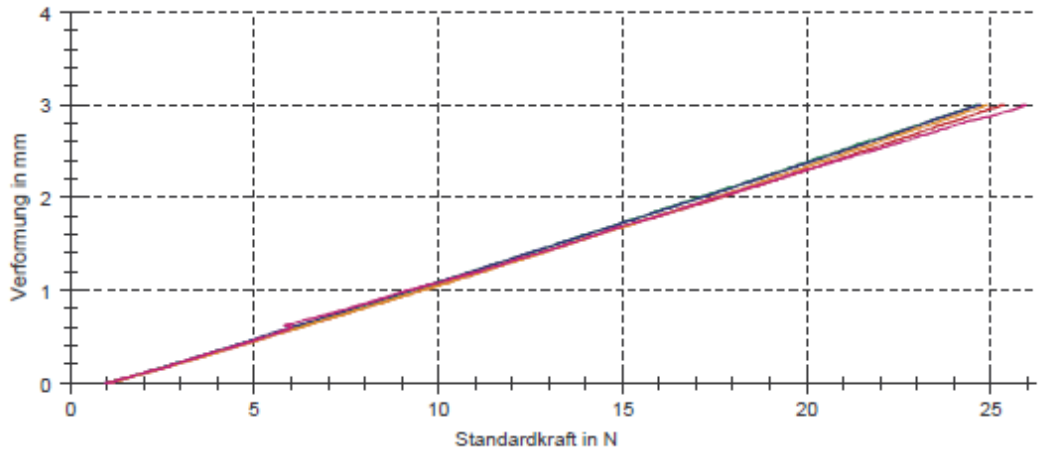

B.3 Zwick protocol for the 3PBT – Strain gage measurement

Zwick / Roell

11.09.18

Prüfprotokoll

Kunde	:	OTH Regensburg	Probentyp	:	
Auftrags-Nr.	:		Vorbehandlung	:	
Prüfnorm	:	DIN EN ISO 14125	Prüfer	:	Andreas Kastenmeier/Max Faber
Art und Bezeichnung	:	FW2-3-Punktbiegeversuche	Bemerkung	:	
Werkstoff	:	FW2 CFK	Maschinendaten	:	
Probenentnahme	:				

Prüfung	:	Verfahren A
Vorkraft	:	1 N
Prüfgeschwindigkeit	:	5 mm/min

Prüfergebnisse:

Nr	Probenkennung	Datum/Uhrzeit	σ_f' MPa	σ_f'' MPa	E_f GPa	σ_{fC} MPa	σ_{fM} MPa	ε_M %	L mm	h mm
9	FW2-B001_119_V4	23.07.2018 10:43:01	0,942	1,462	1,02	-	-	-	106	5,3
10	FW2-B001_119_V4	23.07.2018 10:44:26	0,887	1,401	1,05	-	-	-	106	5,3
14	FW2-B001_119_V4	23.07.2018 11:03:07	0,892	1,393	0,991	-	-	-	106	5,3
15	FW2-B001_119_V4	23.07.2018 11:34:52	0,878	1,398	1,04	-	-	-	106	5,3

Nr	b mm
9	15,2
10	15,2
14	15,2
15	15,2

Seriengrafik:

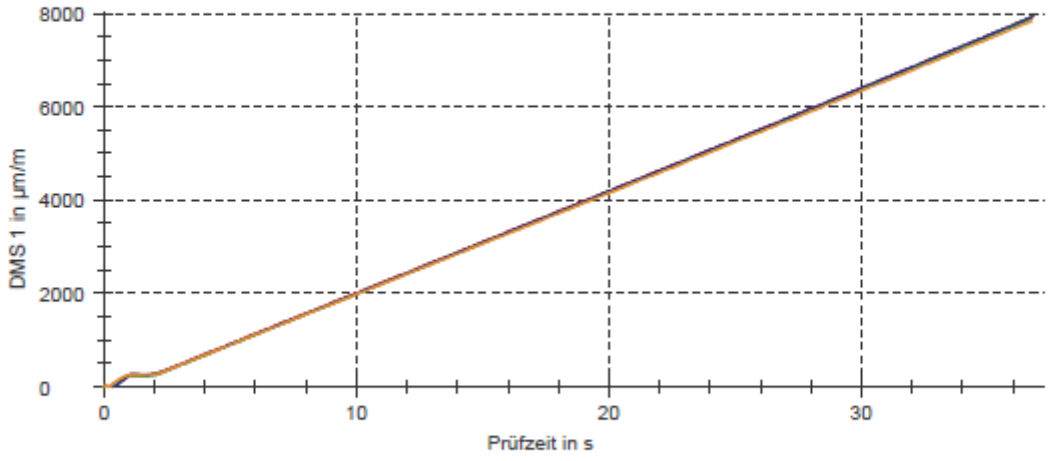

B.4 Zwick protocol for the 4PBT

Zwick / Roell

13.06.18

Prüfprotokoll

Überschrift	:	Prüfprotokoll
Kunde	:	4-Point-Bending - Siegl, Vauge and
Auftrags-Nr.	:	FW2-Druck-50kN
Prüfnorm	:	4-Point-Bending
Art und	:	12-100-D-002-4P
Werkstoff	:	GFRP-Tube
Probenentnahme	:	
Probentyp	:	
Vorbehandlung	:	
Prüfer	:	Siegl
Bemerkung	:	
Maschinendaten	:	
Vorkraft	:	800 N
Prüfgeschwindigkeit	:	1 mm/min

Prüfergebnisse:

Nr	Proben-Nr.	Probenbezeichnung	Probenkennung	Hinweis	Datum/Uhrzeit	L_c mm
1	1		4-Punkt-Biege-Test10KN	erster	13.06.2018	120,00

Nr	L_0 mm	F_{max} N	dL bei mm	W bis Nmm	d_i mm	Rohrlänge mm	S_0 mm²	$t_{Prüfung}$ s
1	120,00	10000	2,5	7506,57	120	1000	1,00	153,57

Seriengrafik:

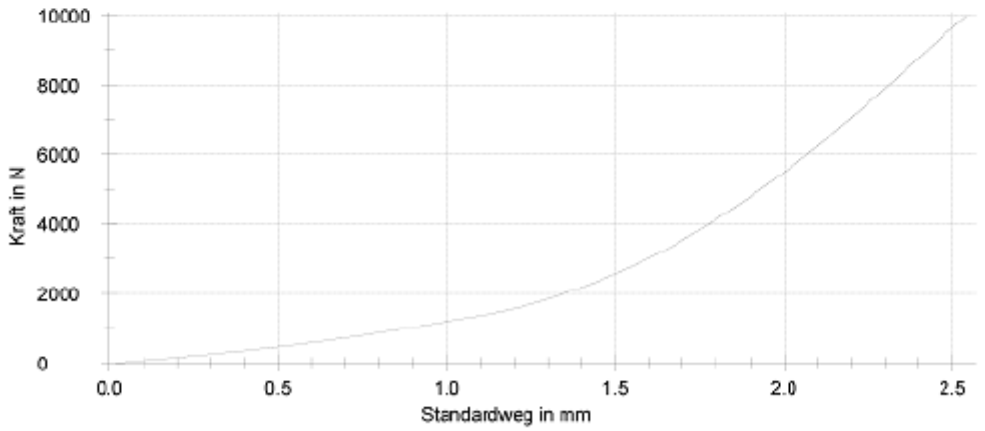

Zwick / Roell

13.06.18

Statistik:

Serie n = 1	Proben-Nr.	L_c mm	L_o mm	F_{max} N	dL bei mm	W bis Nmm	d_i mm	Rohrlänge mm	S_o mm²	$t_{Prüfung}$ s
$\tilde{x}$	1	120,00	120,00	10000	2,5	7506,57	120	1000	1,00	153,57
s	-	-	-	-	-	-	-	-	-	-
V [%]	-	-	-	-	-	-	-	-	-	-

C Final Thesis Presentation

Evaluation of 3D Optical Motion and Deformation Analysis using GOM Aramis 6M Essential Line

Anna Adrover, Bachelor Thesis
Ostbayerische Technische Hochschule Regensburg

Work description

1. Introduction to the GOM ARAMIS System
   - 1.1 Software Description
   - 1.2 Strain Computation
2. Examination Procedure
3. Evaluation test methods
   - 3.1 Simple Cantilever Beam
   - 3.2 Tensile Test
   - 3.3 3 Point Bending Test
4. Evaluation of Aramis on a 4 Point Bending Test
5. Conclusions

Introduction to the GOM ARAMIS Operating System

1.1 Software description

- **Non contact** optical 3D measuring system that computes, analyses and documents object deformations of measuring objects.
- **Stereo camera setup**
- Based on **Digital Image Correlation** principle.

1.2.1 Evaluation of image areas

- **Evaluation of Image Areas via Reference Point Markers**
  - Identification using the contrast at the boundary between black and white.
  - The center point of the elipse is the measuring point (start point).
  - Only capable of measuring displacements.

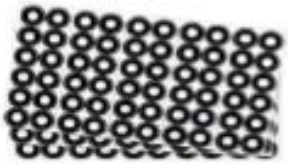

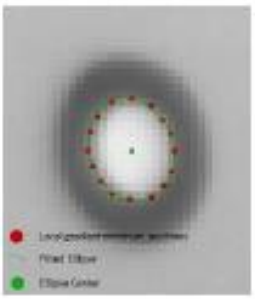

1.2.1 Evaluation of image areas

- **Evaluation of Image Areas via Facets**
  - **Stochastic pattern:** random application of black and white spray.
  - The contribution of black and white spots should be 50/50.
  - Bigger or smaller spots depending on the measured object.

Correct application

Spots too small. Not contrast enough

OTH OSTBAYERISCHE TECHNISCHE HOCHSCHULE REGENSBURG

Introduction to the GOM ARAMIS System:
Digital Image Correlation Working Principle

- **Evaluation of Image Areas via Facets**
  - **Facet:** Squared image areas detected in the stochastic pattern.
  - The center of the square is the identification point.

Main assumption: There is a causal connection between original and deformed state.

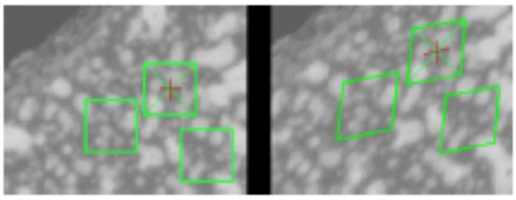

Original vs. Deformed State

$$f(x,y) \overset{!}{\longleftrightarrow} g(x_t, y_t)$$

Correlation Function

$$c(\Delta x, \Delta y) = \frac{\langle f(x,y), g(x+\Delta x, y+\Delta y) \rangle}{|f(x,y)| \cdot |g(x,y)|}$$

Rate of similarity of both signals

OTH OSTBAYERISCHE TECHNISCHE HOCHSCHULE REGENSBURG

Introduction to the GOM ARAMIS System:
Digital Image Correlation Working Principle

1.2.2 Triangulation

- 2 or more signals
- Optical Sensors and sensor calibration
- Camera orientation
- Intrinsic Parameters
- Extrinsic Parameters

1. Strain Computation

1.3.1 Theoretical Definition

Strain: Relative length change of an element.
Stretch Ratio: Quotient between the final length and the initial length.

Technical Strain

$$\varepsilon = \frac{\Delta l}{l_0}$$

Stretch Ratio

$$\Lambda = \frac{l_1}{l_0} = \frac{l_0 + \Delta l}{l_0} = 1 + \varepsilon$$

1.3.2 Stretch Tensor Computation

Continuum mechanics → Kinematic Analysis → Deformation calculated as: $\vec{x} = \chi\left(\vec{X}, t\right)$

$$\vec{x} = \chi\left(\vec{X}, t\right) \xrightarrow{\text{Gradient of the function}} \mathbf{F} := grad\left(\vec{\chi}\left(\vec{X}, t\right)\right) = \frac{d\chi_i}{dX_j}\vec{e}_i \otimes \vec{e}_j = \begin{pmatrix} F_{11} & F_{12} & F_{13} \\ F_{21} & F_{22} & F_{23} \\ F_{31} & F_{32} & F_{33} \end{pmatrix}$$

Deformation Gradient

1.3.2 Stretch Tensor Computation

- The polar decomposition of the Deformation Gradient turns into 2 tensors:

  F = R (Rotation tensor) · **U** (Stretch tensor)

- When transforming the points from the original to the actual state, the stretch is carried out first.

- The Stretch tensor **U** is containing the strains.

$$\mathbf{U} = \begin{pmatrix} \mathbf{U}_{11} & \mathbf{U}_{12} & \mathbf{U}_{13} \\ \mathbf{U}_{21} & \mathbf{U}_{22} & \mathbf{U}_{23} \\ \mathbf{U}_{31} & \mathbf{U}_{32} & \mathbf{U}_{33} \end{pmatrix} = \begin{pmatrix} \Lambda_{11} & \Lambda_{12} & \Lambda_{13} \\ \Lambda_{21} & \Lambda_{22} & \Lambda_{23} \\ \Lambda_{31} & \Lambda_{32} & \Lambda_{33} \end{pmatrix}$$

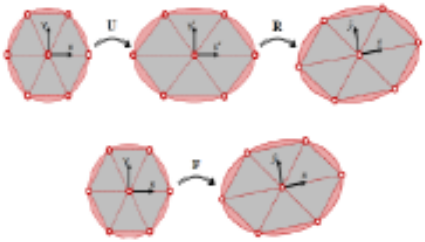

1.3.2 Computation on the software

- Global Coordinate System Initial Position determined during first calibration
- Z-axis as thickness direction.
- Strain in X-axis always computed in material coordinates

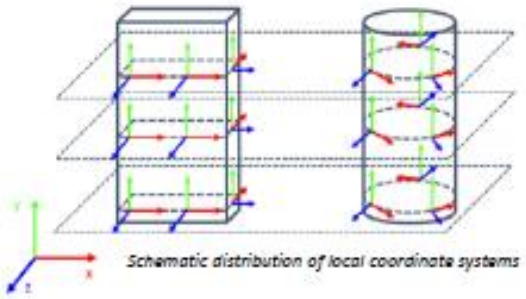

Schematic distribution of local coordinate systems

1.3.2 Computation on the software

- ARAMIS measures points on a surface
- The deformation of this points are calculated as follows:

$$\overrightarrow{p_i}' = \vec{u} + \mathbf{F} \cdot \overrightarrow{p_i} \quad \Leftrightarrow \quad \begin{pmatrix} p_x' \\ p_y' \end{pmatrix} = \begin{pmatrix} u_x \\ u_y \end{pmatrix} + \begin{pmatrix} F_{11} & F_{12} \\ F_{21} & F_{22} \end{pmatrix} \cdot \begin{pmatrix} p_x \\ p_y \end{pmatrix}$$

- 6 unknows → mínimum of 3 points need to be known (traingle)

ARAMIS uses 7 points → **Hexagons** → overdeterminated system of equations

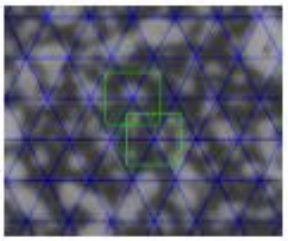

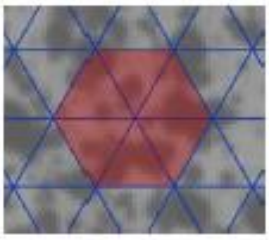

Examination Procedure: From image acquisition to result computation

1.4 Examination Procedure

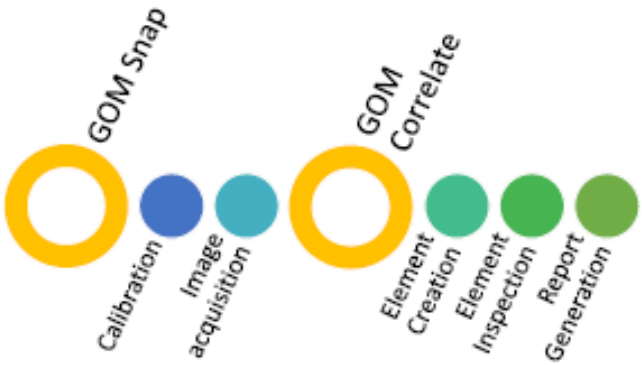

OSTBAYERISCHE TECHNISCHE HOCHSCHULE REGENSBURG

GOM ARAMIS 6M Essential.
Examination Procedure

GOM Snap. Calibration

Sensor Set Up
- Equip cameras
- Ajust slider distance
- Ajust focus
- Ajust Aperture
- Angle 25°

Sensor Warm Up
- 15 min required

Sensor Calibration
- Calibration Plate

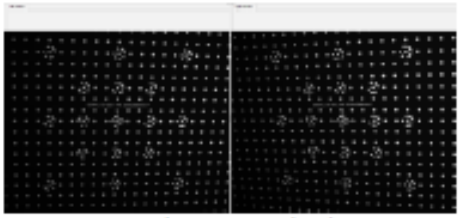

Left and right Camera Calibration

Example of the small plate calibration

OSTBAYERISCHE TECHNISCHE HOCHSCHULE REGENSBURG

GOM ARAMIS 6M Essential.
Examination Procedure

GOM Snap. Calibration

Calibrated sensor

Sensor name	ARAMIS Adjustable Base
Measuring volume	Adjustable measuring volume
Camera support	Adjustable base 500
Working distance	660 mm
Camera angle	25°
Camera distance	256 mm
Serial number	no identifier

Determined by the user

Calibration Result

Calibration deviation	0.018 Pixels
Calibration deviation (check)	OK (limit value: 0.050 Pixels)
Scale deviation	0.024 mm
Scale deviation (check)	OK (limit value: 0.031 mm)
Camera angle	25.4°
Height variance	220 mm
Measuring volume	315 / 260 / 260 mm → (Weight /Height /Field)

Succesful calibration

OTH Ostbayerische Technische Hochschule Regensburg

GOM ARAMIS 6M Essential.
Examination Procedure

GOM Snap. Image Acquisition

1. Initialize sensors
2. Set a low time computation so that theres is no execessive brightness
3. Set the desired image frequency
4. Record first between 20-40 static pictures for noise measurment.
5. Record experiment

Example of a correct time computation for a tensile test

OTH Ostbayerische Technische Hochschule Regensburg

GOM ARAMIS 6M Essential.
Funcionament dels programas

GOM Correlate.

- **Element creation**
  1. **Surface Component**
     - Surface Computation
     - Facet dimensions
     - Facet distance
     - Starting Facet
  2. **Alignment**
     - 3-2-1 Alignment
     - 3 point Alignment using a CAD imported file

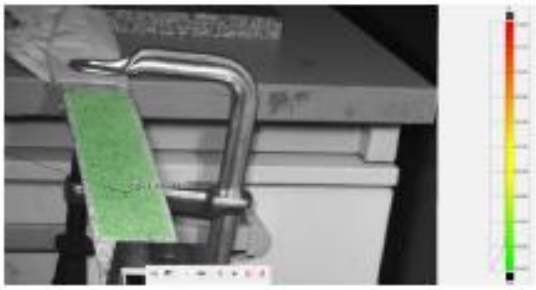

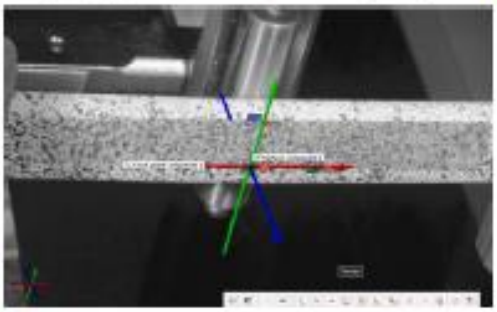

OTH Ostbayerische Technische Hochschule Regensburg

Evaluation Test Methods:
Simple Cantilever Beam

Simple Cantilever Beam

Aluminium Beam: 2x50x377 mm

Calibration parameters

- **Measuring distance:** 690mm
- **Slider distance:** 270 mm
- **DOF:** 270 mm

Force applied: 11,6 N

Pattern Applied: Stochastic Pattern

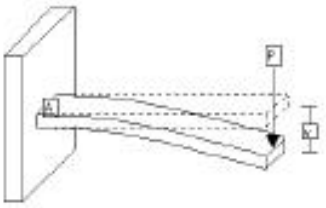

OTH Ostbayerische Technische Hochschule Regensburg

Evaluation Test Methods:
Simple Cantilever Beam

Simple Cantilever Beam. Inspection

- Surface Creation: Standard Computation
- 3-2-1 Aligment

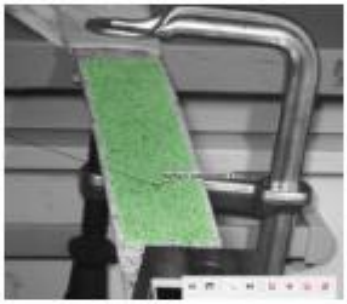

Good quality pattern

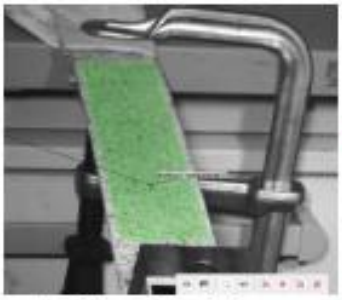

Low intersection deviation

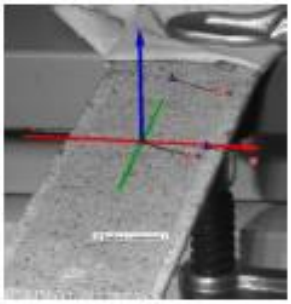

Correct aligment

OTH OSTBAYERISCHE TECHNISCHE HOCHSCHULE REGENSBURG

Evaluation Test Methods:
Simple Cantilever Beam

Simple Cantilever Beam. Results

- Z displacements Computed.

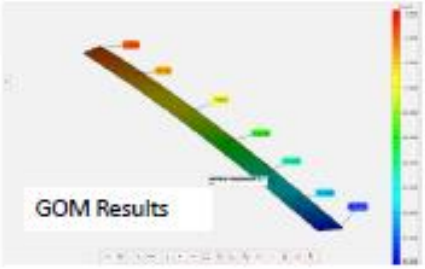

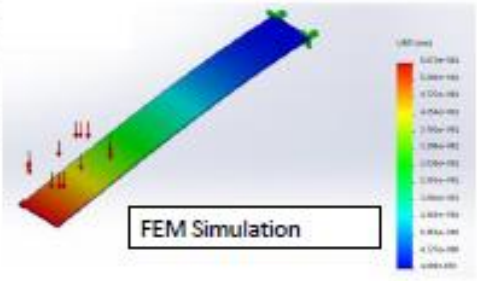

OTH OSTBAYERISCHE TECHNISCHE HOCHSCHULE REGENSBURG

Evaluation Test Methods:
Tensile Test

Tensile Test

Specimens
- Polyoxymethylene (POM)
- 5 units

Test Setup
- Universal Test Machine
- Clamping Grid system rotated 45°.
- Extensometers
- Max. Strain limited 2.5%

Calibration parameters
- **Measuring distance:** 660 mm
- **Slider distance:** 256mm
- **DOF:** 260mm

Pattern Applied: Stochastic Pattern

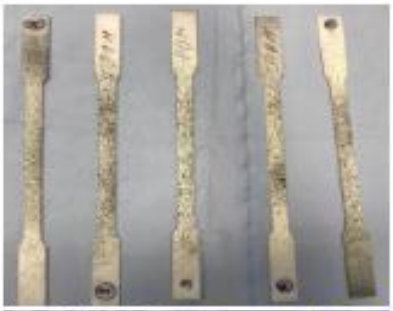

OTH OSTBAYERISCHE TECHNISCHE HOCHSCHULE REGENSBURG

Evaluation Test Methods:
Tensile Test

Tensile Test

Element Creation:

- Surface Component. Standard Computation
- 3-2-1 Alignment

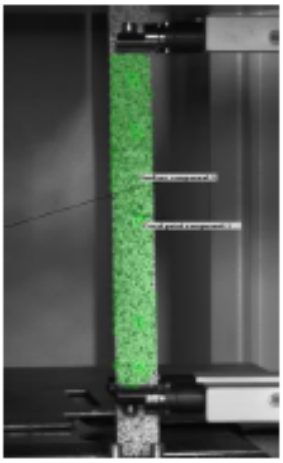

Good quality pattern

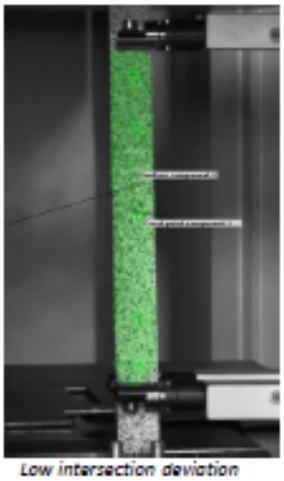

Low intersection deviation

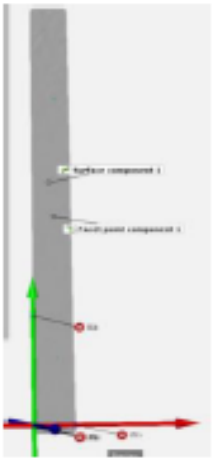

Correct aligment

OTH OSTBAYERISCHE TECHNISCHE HOCHSCHULE REGENSBURG

Evaluation Test Methods:
Tensile Test

Tensile Test. Result Comparison

	d= 660mm	d = 810 mm
	Epsilon y	Epsilon y
Average Value (%)	2,498	2,497
Standard Deviation	0,014	0,016
Absolut Error	0,002	0,003

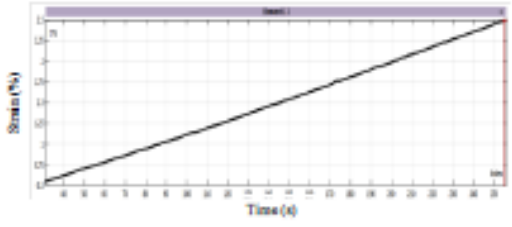

GOM Results

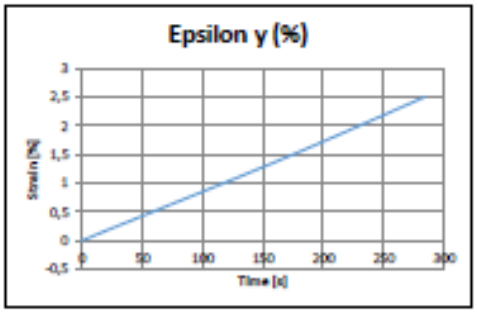

Zwick Machine Results

OTH OSTBAYERISCHE TECHNISCHE HOCHSCHULE REGENSBURG

Evaluation Test Methods. 3 Point Bending Test

3 Point Bending Test

Specimens

- Polyoxymethylene (POM)
- ISO 178

Test Setup

- Universal Test Machine
- 3 Point Bending Test installed
- Strain Gage – One direction (Ex)
- Max. displacement 3mm

Calibration parameters

- **Measuring distance:** 360 mm
- **Slider distance:** 140 mm
- **DOF:** 125 mm

Pattern Applied: Stochastic Pattern

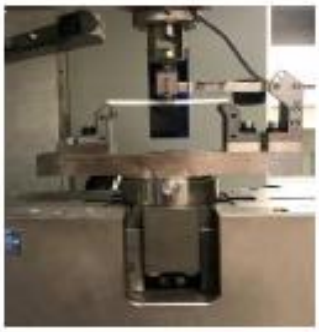

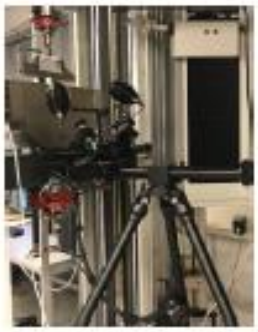

OTH OSTBAYERISCHE TECHNISCHE HOCHSCHULE REGENSBURG

Evaluation Test Methods. 3 Point Bending Test

3 Point Bending Test

Element Creation:

- Surface Component. More points Computation
- 3-2-1 Alignment

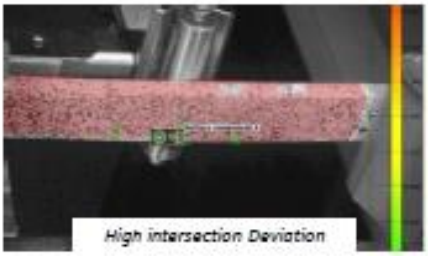

High intersection Deviation

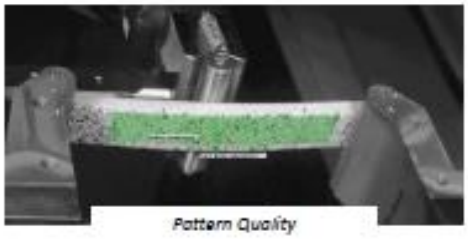

Pattern Quality

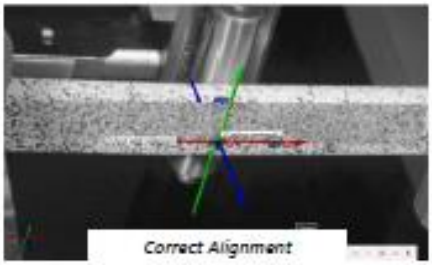

Correct Alignment

OTH Ostbayerische Technische Hochschule Regensburg

Evaluation Test Methods.
3 Point Bending Test

3 Point Bending Test. Results Comparison

1. GOM ARAMIS
Average value of $\varepsilon = 0{,}947\ \%$
Standard deviation = 0,006

2. Strain Gages
Average value of $\varepsilon = 0{,}788\ \%$
Standard deviation = 0,008

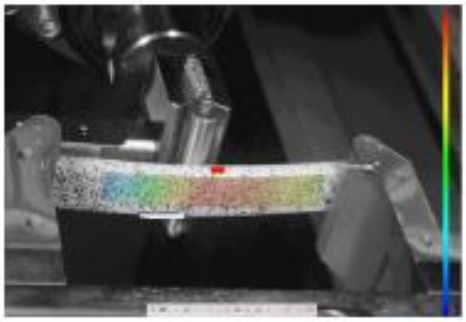

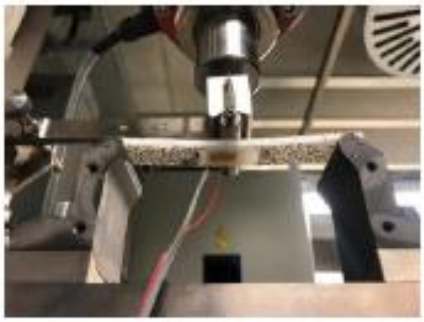

Absolut Error = 0,16

OTH Ostbayerische Technische Hochschule Regensburg

Evaluation Test Methods.
3 Point Bending Test

3 Point Bending Test. Results Comparison

GOM Results:

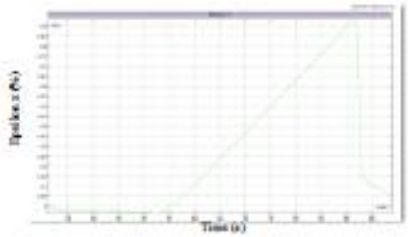

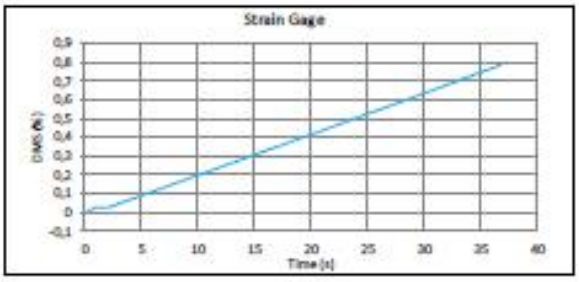

OSTBAYERISCHE TECHNISCHE HOCHSCHULE REGENSBURG

LFT

Evaluation of GOM Aramis on the 4 Point Bending Test

Anna Adrover
Marco Siegl, M.Sc. Prof. Dr.-Ing. Ingo Ehrlich

4 Point Bending Test

Specimen

- Fiber Reinforced plastic composite tube
- D_{outer} = 133 mm

Test Setup

- Universal Test Machine
- 4 Point Bending Test Setup
- DMS at 45° bi-directional
- 10 kN Force Applied

Calibration parameters

- **Measuring distance:** 690 mm
- **Slider distance:** 270 mm
- **DOF:** 290 mm

Pattern Applied: reference point markers and stochastic pattern

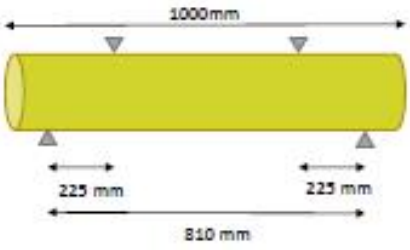

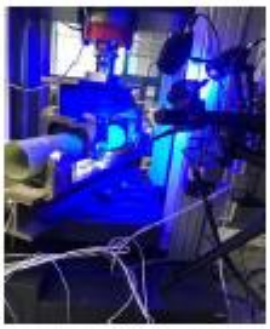

Anna Adrover
Marco Siegl, M.Sc. Prof. Dr.-Ing. Ingo Ehrlich

LFT

OTH OSTBAYERISCHE TECHNISCHE HOCHSCHULE REGENSBURG

Evaluation of GOM Aramis on the 4 Point Bending Test

4 Point Bending Test

Element Creation:

- Surface Component. Standard Computation
- 3 points Alignment – CAD File imported.

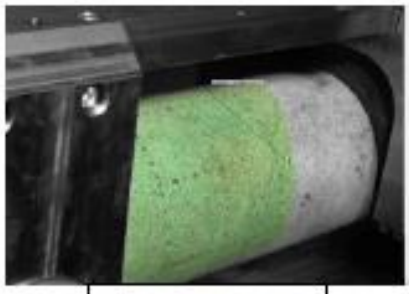

Intersection Deviation

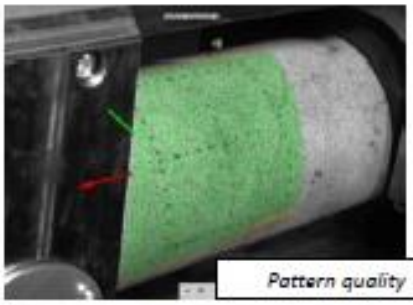

Pattern quality

Alignment

OTH OSTBAYERISCHE TECHNISCHE HOCHSCHULE REGENSBURG

Evaluation of GOM Aramis on the 4 Point Bending Test

4 Point Bending Test. Results

- Strain Computation not possible due to the noise.

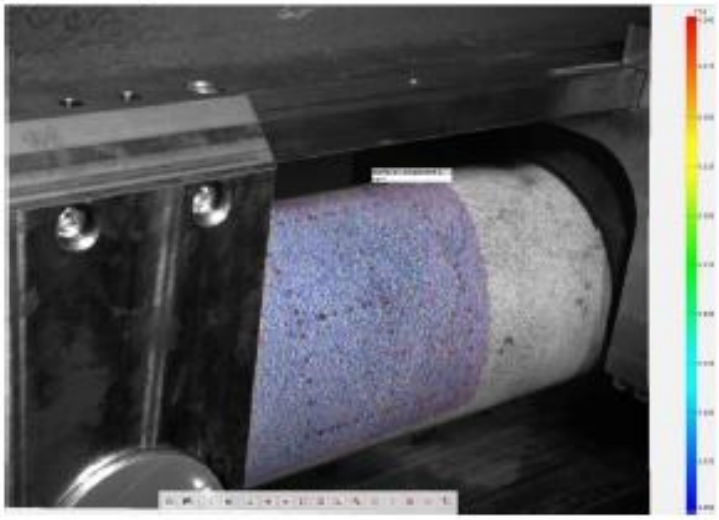

OTH Ostbayerische Technische Hochschule Regensburg

Evaluation of GOM Aramis on the 4 Point Bending Test

4 Point Bending Test. Results

- Displacement computation in Z direction:

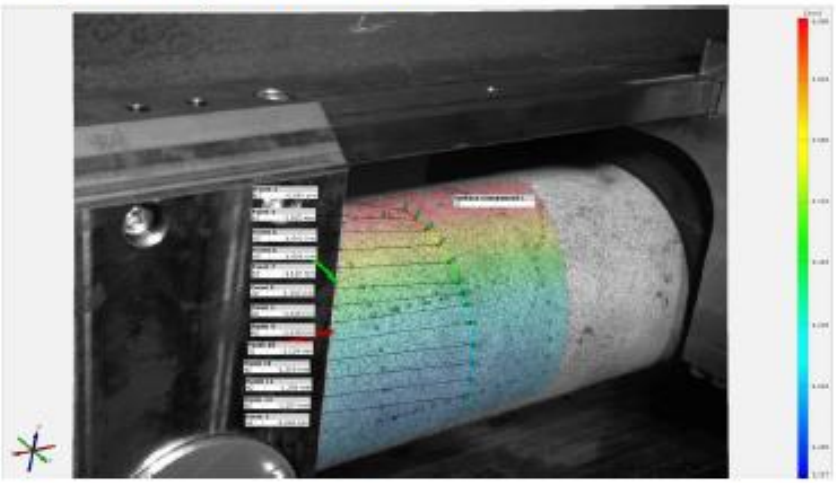

OTH Ostbayerische Technische Hochschule Regensburg

Evaluation of GOM Aramis on the 4 Point Bending Test

4 Point Bending Test. Results

- Displacement computation in Y direction:

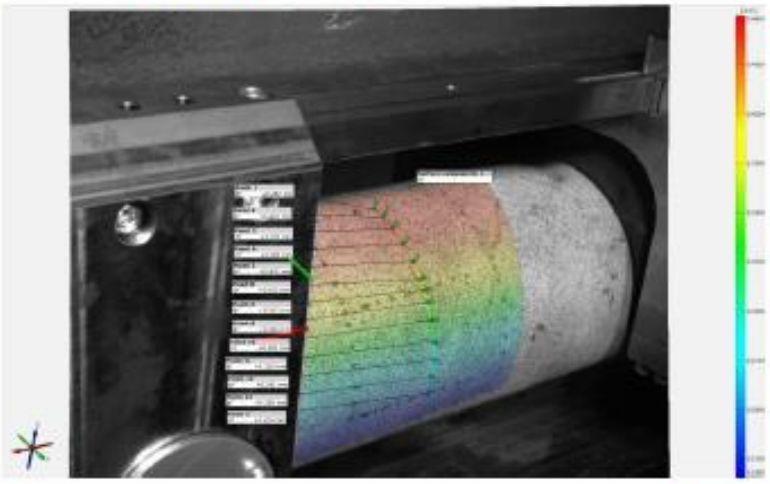

Analytical suppression of the rotation

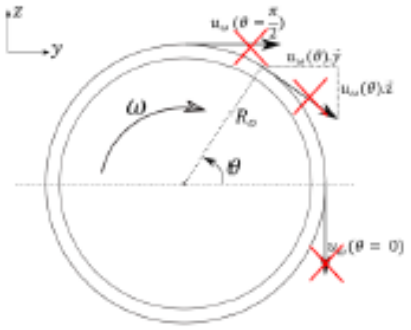

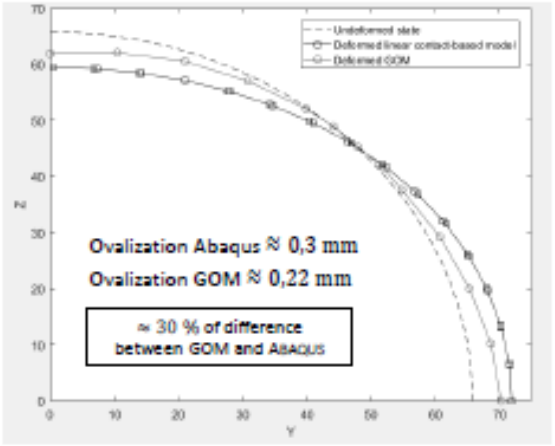

Conclusions

- Strain computation up to 0.1% .
- Lower intersection deviation ensures better results.
- Moving the cameras between the DOF range will not alter significantly the results.

Further Work

- Analysis of the 4PBT with the new rubber (1.5 mmm thickness)
- Higher Forces to obtain measurable strains with the GOM System
- Assembly of a support inside the universal test machine.

References

1. N.N.: *GOM Acqusition Basic* – Aramis Manual GOM, 2016.
2. N.N.: *GOM Adjustable Base*- Aramis Manual GOM, 2016
3. N.N.: *GOM Testing* – Aramis Manual GOM, 2016
4. N.N.: *EN 178:2010:E Plastics – Deformation of Flexural Properties*. March 2013.
5. Vauge, A. (2018). *Bending behavior of fiber-reinforced plastic tubes 4-point bending tests* (Non published Presentation). Ostbayerische Technische Hochschule Regensburg, 2018

Thanks for your attention

D Media Content

The CD in this document does not contain all the examined data required for its development, due to the fact that the GOM files are heavy and the CD does not have the needed space for storing all the file. It has been possible just to storage the whole information (calibration protocols, FEM simulation file and GOM files) regarding the Cantilever Beam Test and the 3-Point Bending Test.
Therefore, for all the remaining test the only available information that can be found in the CD are the GOM calibration protocols and the universal machine protocols.
In addition, there is the final PDF copy of this present document and the PDF final presentation.

The whole volume data is uploaded in the LFT server (http://172.20.30.152:500), following the order shown in the next figure:

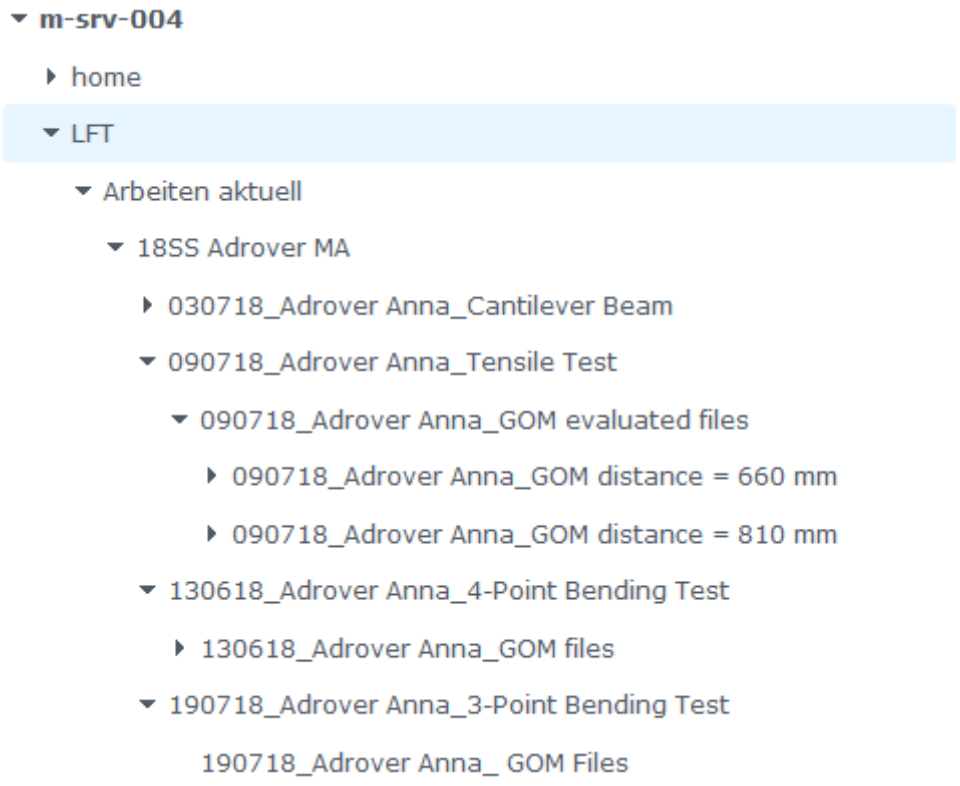

D Media Content